Improving the potency and reducing the susceptibility to MDR resistance of combretastatins by means of 3-substituted indole moieties.

Substitution at the indole 3 position yields highly potent indolecombretastatins with reduced susceptibility to MDR resistance.

Raquel Álvarez,[†,#,≠,§] Consuelo Gajate,[‡,§] Pilar Puebla,[†,#,≠] Faustino Mollinedo,[‡] Manuel Medarde[†,#,≠] and Rafael Peláez[,†,#,≠]*

[*] To whom correspondence should be addressed. Telephone: 34 677 554890. E-mail: pelaez@usal.es

[†] Laboratorio de Química Orgánica y Farmacéutica

[#] Laboratory of Cell Death and Cancer Therapy, Department of Molecular Biomedicine, Centro de Investigaciones Biológicas, Consejo Superior de Investigaciones Científicas (CSIC), E-28040 Madrid, Spain

[#] Instituto de Investigación Biomédica de Salamanca (IBSAL)

[≠] Centro de Investigación de Enfermedades Tropicales de la Universidad de Salamanca (CIETUS).

[†] Universidad de Salamanca. Laboratorio de Química Orgánica and Farmacéutica. Departamento de Ciencias Farmacéuticas. Campus Miguel de Unamuno. E-37007. Salamanca. Spain.; [‡]Laboratory of Cell Death and Cancer Therapy, Department of Molecular Biomedicine, Centro de Investigaciones Biológicas, Consejo Superior de Investigaciones Científicas (CSIC), E-28040 Madrid, Spain; [#] Instituto de Investigación Biomédica de Salamanca (IBSAL) and [≠] Centro de Investigación de Enfermedades Tropicales de la Universidad de Salamanca (CIETUS).

RECEIVED DATE

Abstract: Resistance to combretastatin A-4 is mediated by metabolic modification of the phenolic hydroxyl and ether groups of the 3-hydroxy-4-methoxyphenyl (B ring). Replacement of the B ring of combretastatin A-4 by a *N*-methyl-5-indolyl reduces tubulin polymerization inhibition (TPI) and cytotoxicity against human cancer cell lines but cyano, methoxycarbonyl, formyl, and hydroxyiminomethyl substitutions at the indole 3-position restores potent TPI and cytotoxicity against sensitive human cancer cell lines. These highly potent substituted derivatives displayed low nanomolar cytotoxicity against several human cancer cell lines due to tubulin inhibition, as shown by cell cycle analysis, confocal microscopy, and tubulin polymerization inhibitory activity studies and promoted cell killing mediated by caspase-3 activation. Binding at the colchicine site was suggested by molecular modeling studies. Substituted combretastatins displayed higher potencies than the isomeric isocombretastatins and the highest potencies were achieved for the hydroxyiminomethyl (**21**) and cyano (**23**) groups, with TPI values in the submicromolar range and cytotoxicities in the subnanomolar range. Dose-response and time-course studies showed that drug concentrations as low as 1 nM (**23**) or 10 nM (**21**) led to a complete G_2/M cell cycle arrest after 15 h treatment followed by a high apoptosis-like cell

[§] These authors contributed equally to this work.

response after 48-72 h treatment. The P-glycoprotein and calcium antagonist verapamil increased **21** and **23** cytotoxicity to IC_{50} values of 10^{-10} M, and highly potentiated the cytotoxic activity in 100-fold of the CHO derivative (**17**), in A549 human non-small cell lung cancer cells. The differences in cytotoxic potency observed between the highly potent cyano (**23**) and hydroxyiminomethyl (**21**) groups and other substituents with similar TPI values (**17**) were very much reduced upon co-treatment with verapamil. A 3,4,5-trimethoxyphenyl ring always afforded more potent derivatives than a 2,3,4-trimethoxyphenyl ring.

INTRODUCTION

Microtubules and their main constituents the αβ-tubulin heterodimers are the targets of many anti-tumor and anti-parasitic drugs that disrupt their dynamical equilibrium. Microtubule-targeting agents (MTAs) can affect cell shape maintenance, trafficking, cilia and flagella functioning, signaling, and mitosis as some of the many functions of microtubules in the cells. Several drug binding sites different from the nucleotide binding sites have been described, with at least seven structurally characterized, including the taxanes, the vinca alkaloids, the colchicine, the laulimalide/peloruside, the maytansine, the pironetin, and the hemiasterlin sites located in both the α and β tubulins. Some MTA stabilize the microtubules, as for example paclitaxel, while other destabilize them, as for instance colchicine, but at low concentrations all of them affect the polymerization/depolymerization dynamics.[1]

The pivotal role of microtubules in mitosis, together with their role as scaffolds for signaling molecules modulating apoptosis, makes them a major target in cancer chemotherapy, and thus MTAs lead to cell cycle arrest at G_2/M phase and late apoptosis.[2] Inhibition of the mitotic spindle is the most common signature of MTAs in cell treatment, and therefore they are often referred to as anti-mitotic agents, although other mechanisms are probably important in their in vivo anti-tumor effects.[3, 4] In fact, colchicine site binding drugs as for instance the combretastatins (Figure 1) are often considered vascular disrupting agents (VDA), because in vivo they cause a rapid collapse of the tumor associated

vasculature and blood flow shutdown which is mainly responsible for tumor death.[5, 6] The emergence of VDAs holds great potential in the treatment of malignant solid tumors, and the 3-O-phosphate prodrug of combretastatin A-4 (CA4P), the more effective CA1P (Oxi4503) and the amino analogue AVE8062 are undergoing preclinical and clinical development.[7] However, despite a rapid initial central tumor necrosis after VDAs treatment, a peripheral rim of resistant viable cancer cells remains and eventually grow to the necrotic area causing recurrence and metastasis.[8, 9] Several strategies have been applied to increase the clinical efficiency of combretastatins, including combinations with antiangiogenic drugs or with other antitumor agents or the development of more potent derivatives.

Figure 1. Representative combretastatin type ligands

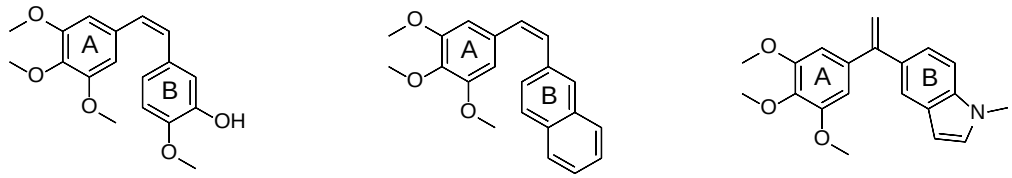

Combretastatin A-4 (CA4) Naphthylcombretastatins Indoleisocombretastatin

Innate or acquired resistance mechanisms employed by cancer cells against treatment with combretastatin A-4 have been described, including adaptation to the hypoxic conditions and reestablishment of the vasculature in response to the reduction in blood supply as well as direct resistance to the drug. The B ring of combretastatin A4 through its hydroxyl group provides the attachment point for prodrug formation thus allowing pharmacokinetic optimization but it is also its Achilles´ heel struck by phase I and II metabolic reactions associated with its inactivation, as shown for resistant hepatocellular carcinoma or colon adenocarcinoma-derived HT-29 cells.[10-12]

We have previously shown that an indole ring is a suitable replacement for the B ring of combretastatin A4 in the context of a 1,1-diarylethene (isocombretastatin) skeleton (Fig. 1).[13] Substitutions of the indole 3 position did not result in improvements with respect to the parent unsubstituted indole. Surprisingly, the isomeric indole combretastatin (1,2-diarylethene) showed much lower potency.[14] Here we show that introduction of substituents at the 3 position of indole combretastatin improves on the tubulin inhibitory

activity. Furthermore, the cytotoxicity of compounds with similar tubulin inhibitory potency against combretastatin A4 resistant colon adenocarcinoma (HT-29) and lung adenocarcinoma (A-549) cell lines is dependent on minor structural changes and can be further improved upon combination with verapamil. Our results suggest that MDR efflux is an important factor in the observed cytotoxicity differences and that substitution at the indole 3 position with appropriate substituents such as the cyano or hydroxyimino groups greatly reduces the compounds' efflux and result in apoptotic-like cell death after complete G_2/M cell cycle arrest after very low dose (1nM) drug treatments.

RESULTS AND DISCUSSION

Chemical synthesis

The synthesis of combretastatins was carried out by the usual Wittig procedure, followed by derivatization at 3-position of the indoles. The indole aldehydes used as starting materials **1**-**5**, were obtained from commercial 1*H*-indole-5-carboxaldehyde (Scheme 1), whereas 1*H*-benzo[*d*]imidazole-5-carboxylic acid (**6**) was used to prepare the corresponding 1-methyl-1*H*-benzo[*d*]imidazole-5(6)-carbaldehydes (**9** and **10**, Scheme 2). Indole-combretastatins unsubstituted at 3-position **13**, **15**[14] and **16** were respectively synthesized by Wittig olefination of **1** and **2** with 3,4,5-trimethoxybenzyl bromide (**11**) and **2** with 2,3,4-trimethoxybenzyl bromide (**12**) (Scheme 1). **15** and **16** were readily formylated at 3-position,[15] to yield **17** and **18** (Scheme 3), the two latter used to prepare derivatives at this position **19**-**34**.

To complete the series of compounds to assay, the aldehyde **14**, bromoderivatives **35** and **36** (Scheme 1), and the benzimidazole-combretastatins (Scheme 2) seemed adequate to fulfil the structural modifications of indole related derivatives. The unresolved mixture of 1-methyl-1*H*-benzimidazole-5(6)-carbaldehydes (**9**+**10**), obtained by methylation of 1*H*-benzimidazole-5(6)-carbaldehyde (**8**), was used to produce the combretastatins **37+38**/***Z***+***E***, which could only be partially separated into **37+38**/***Z*** and **37+38**/***E***.

Once separated from the *E*-aldehydes, several transformations aimed at increasing solubility by means of additional nitrogen or oxygen atoms were made, *Z*-aldehydes **17** and **18** were reduced to the alcohols **19** and **20**, transformed into the oximes[16, 17] **21** (***Z***+***E***) and **22** (***Z***+***E***) and oxidized to carboxylic acids[18] **25** and **26**. In addition, the oximes by treatment with acetic anhydride in pyridine, were converted into the nitriles **23** and **24** and the carboxylic acid **25** was transformed into its methyl ester **27**.

Scheme 1: Synthesis of 3-indolecarbaldehyde combretastatin derivatives 13-16 and bromoderivatives 35 and 36.[a]

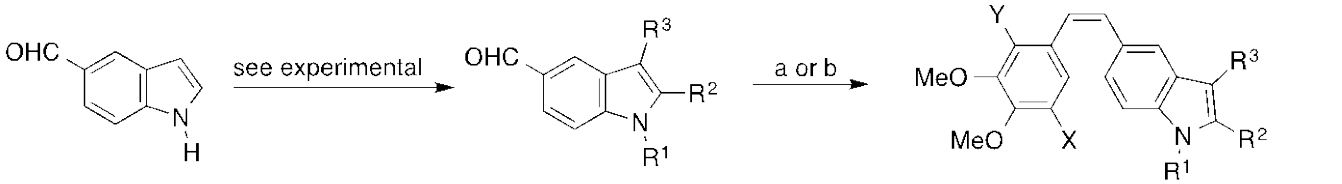

1: R^1=Et, R^2=R^3=H
2: R^1=Me, R^2=R^3=H
3: R^1=Et, R^2=H, R^3=CHO
4: R^1=Me, R^2=H, R^3=Br
5: R^1=Me, R^2=R^3=Br

13: X=OMe, Y=H, R^1=Et, R^2=R^3=H
14: X=OMe, Y=H, R^1=Et, R^2=R^3=CHO
15: X=OMe, Y=H, R^1=Me, R^2=R^3=H
16: X=H, Y=OMe, R^1=Me, R^2=R^3=H
35: X=OMe, Y=H, R^1=Me, R^2=H, R^3=Br
36: X=OMe, Y=H, R^1=Me, R^2=R^3=Br

(a) (i) $(3,4,5\text{-}(MeO)_3PhCH_2)Ph_3PBr$ (**11**), THF, BuLi (1.6M), THF, -40ºC, 1h; (ii) 1-ethyl-1*H*-indole-5-carbaldehyde (**1**), 1-methyl-1*H*-indole-5-carbaldehyde (**2**), 1-ethyl-1*H*-indole-3,5-dicarbaldehyde (**3**), 1-methyl-3-bromo-1*H*-indole-5-carbaldehyde (**4**) or 1-methyl-2,3-dibromo -1*H*-indole -5-carbaldehyde (**5**), THF, -40 ºC to rt, 24 h. (b) (i) $(2,3,4\text{-}(MeO)_3PhCH_2)Ph_3PBr$ (**12**), THF, BuLi (1.6M), THF, -40ºC, 1h; (ii) 1-methyl-1*H*-indole-5-carbaldehyde (**2**), THF, -40 ºC to rt, 24 h.

Scheme 2: Preparation of benzimidazole combretastatin derivatives 37+38.[a]

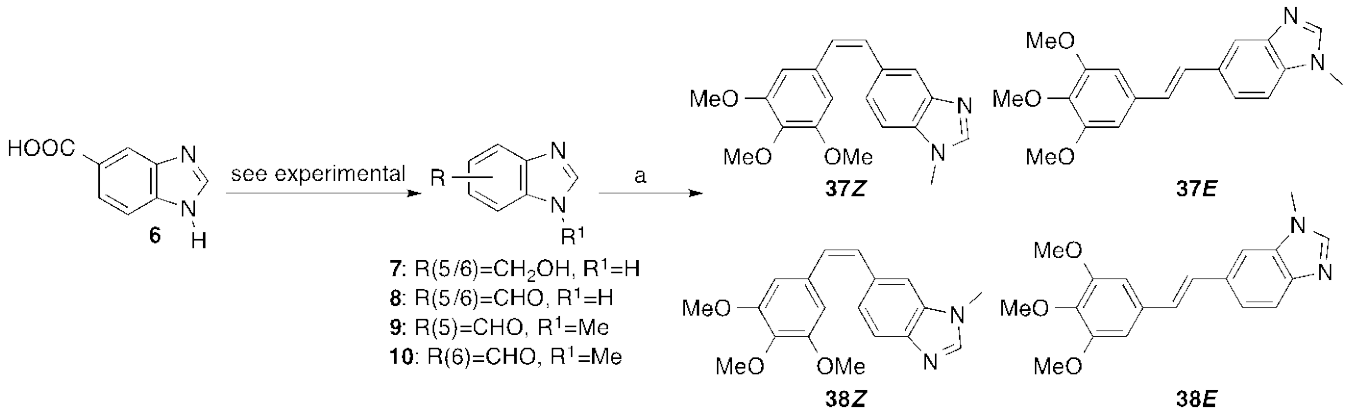

Reagents and conditions: (a) (i) $Ph_3P(3,4,5\text{-}MeO_3PhCH_2)I$, THF, *n*BuLi (1.6M), THF, -40 ºC, 1h; (ii) 1-methyl-1*H*-benzimidazole-5(6)-carbaldehydes, THF, -40 ºC to rt, 24 h.

Scheme 3: Preparation of 3-substituted indole-combretastatin derivatives 17-34.[a]

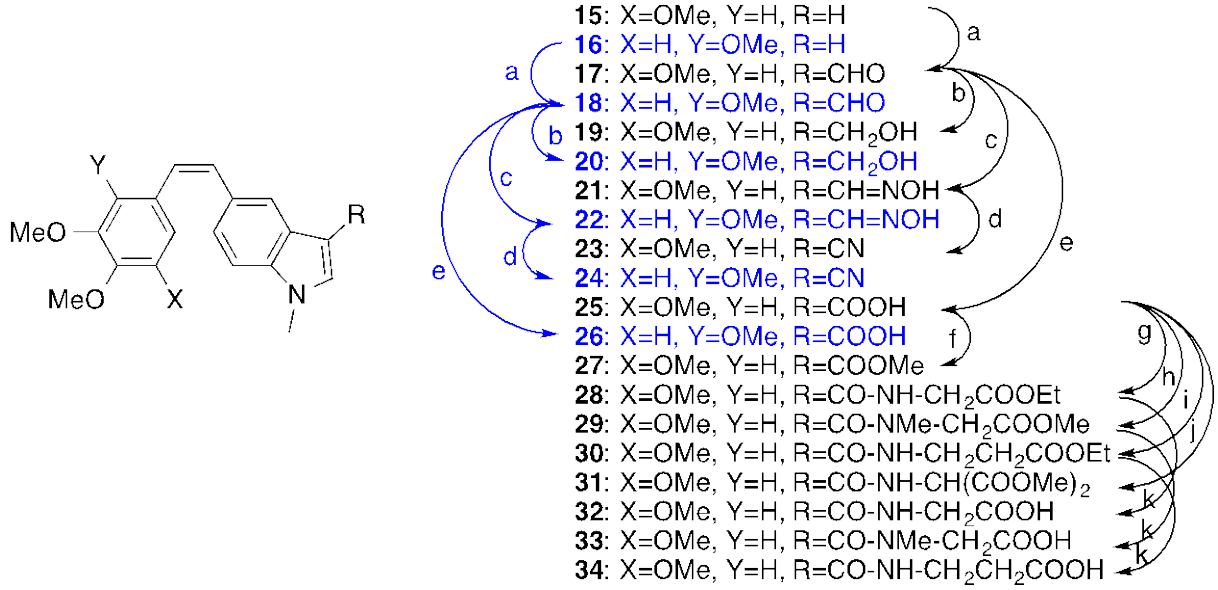

Reagents and conditions: (a) (i) $POCl_3$, DMF, 0 ºC, 1 h; (ii) **15** or **16**, 60 ºC, 2 h. (b) $NaBH_4$, MeOH, rt, 30 min. (c) $NH_2OH{\cdot}HCl$, MeOH, pyr (2 drops), rt, 24 h. (d) Ac_2O, pyr, rt, 4 h. (e) **17** or **18** in *t*BuOH, 2-methyl-2-butene, THF; add $NaClO_2$, NaH_2PO_4, H_2O, rt, 12 h. (f) $TMSCHN_2$, MeOH, 15 min. (g) (i) $NH_2CH_2COOEt{\cdot}HCl$; EDCI; 4-DMAP; rt, 48 h, inert atmosphere. (h) $CH_3NHCH_2COOMe{\cdot}HCl$; EDCI; 4-DMAP; rt, 48 h, inert atmosphere. (i) $NH_2CH_2CH_2COOEt$; EDCI; 4-DMAP; rt, 48 h, inert atmosphere. (j) $(COOMe)_2CHNH_2{\cdot}HCl$; EDCI; 4-DMAP; rt, 48 h, inert atmosphere. (k) KOH/MeOH, rt, 30 min.

Other transformations include the formation of several amides from the carboxylic acid **25**, using different aminoesters (Scheme 3).[19] Thus, the amides **28, 29, 30** and **31** were obtained by treatment with glycine ethyl ester, sarcosine methyl ester, β-alanine ethyl ester and dimethyl aminomalonate. By saponification with KOH/MeOH the carboxylic acids **32**, **33** and **34** were obtained.

With these compounds, representative structures of the 3-substituted 1-methyl-1*H*-indole combretastatins were at hand in order to explore the effect of this substitution on their activities.

Aqueous solubility

Aqueous solubility in phosphate buffer at pH 7.0 was determined using a shake-flask method, microfiltration and UV absorbance measurement of soluble compound. *N*-methylindole combrestatatins with hydrogen at C-3 (**13**, **15** and **16**) display aqueous solubility similar to Combretastatin A-4 (Table 1). Cyano or bromine substituents do not improve aqueous solubility but a carboxylic acid or amides of aminoacids increase the solubility between 40 and 150 times.

Table 1. Aqueous solubility of representative compounds in aqueous buffer pH 7.0

Compound	**Solubility (μg/mL)**	**Compound**	**Solubility (μg/mL)**
CA-4	1.04[20]	**25**	80.0
13	2.0	**27**	1.0
15	2.6	**29**	60.0
16	2.0	**33**	380.0
17	6.0	**34**	352.0
19	3.0	**35**	2.0
23	1.0	**36**	<1.0

Biology.

The effect of the synthesized compounds on cell viability against four types of human cancer cell lines: A-549 human lung carcinoma, HeLa human cervix epithelioid carcinoma, HL-60 human acute myeloid leukemia, and HT-29 human colon adenocarcinoma was assayed by the XTT method.[21] The results are summarized in Table 2. The compounds are cytotoxic at concentrations between micromolar

and subnanomolar, thus indicating that the combination of a trimethoxyphenyl and a 5-indolyl forming a Z stilbene skeleton is a very favorable scaffold for cytotoxicity. The most potent compounds of the series inhibited proliferation of the indicated human cancer cell lines at very low drug concentrations, with IC_{50} values in the 10^{-9} M and 10^{-10} M range. These IC_{50} values were up to 10−100 times lower than those shown by doxorubicin (IC_{50} at a range of 10−8 M). For most compounds the IC_{50} are similar for HL60 and HeLa whereas they are higher for A-549 and HT-29, a difference in sensitivity which has been previously observed for other colchicine site ligands.[10, 13]

Table 2. Tubulin Polymerization Inhibitory Activity, Cytotoxic Activity against Human Cancer Cell Lines, and Results of the Docking Studies.

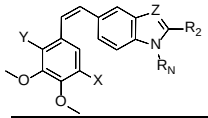

	R_N	**X**	**Y**	**Z**	**R_2**	**%TPI (at 20 *μM*)**[a]	**TPI IC_{50}**[b]	HL-60 (10^{-6} M)[c]	A-549 (10^{-6} M)[c]	HeLa (10^{-6} M)[c]	HT-29 (10^{-6} M)[c]	Binding E (Cluster number // % of conf)[d]
13	Et	OMe	H	CH	H	95	2.0	0.172	0.919	0.27	0.434	-10.31 (1//93)
14	Et	OMe	H	C-CHO	H	95	1.2	0.03	>10	0.029	3.10	-10.40 (1//65)
15	Me	OMe	H	CH	H		2.0		0.47		0.36	-9.80 (1//96)
16Z	Me	H	OMe	CH	H	100[a]	>5	0.0059	1.7	0.062	0.086	-9.24 (2//41)
16E	Me	H	OMe	CH	H	59	4-5	0.0039	0.0046	0.0066	0.0058	
17	Me	OMe	H	C-CHO	H	98	0.5	0.0065	4.7	0.00073	0.6	-10.34 (1//85)
18	Me	H	OMe	C-CHO	H	97	>5	0.0087	7.9	0.043	0.6	-9.74 (2//23)
19	Me	OMe	H	C-CH_2OH	H	91	1.2	0.028	0.045	0.032	0.033	-10.47 (1//79)
20	Me	H	OMe	C-CH_2OH	H	45	≈20	8.5	3.9	1.2	1.0	-9.62 (2//20)
21	Me	OMe	H	C-CH=NOH	H	100	0.5	0.00035	0.002	0.00014	0.0002	-10.93 (E) (1//20) -11.10 (Z) (1//13)
22	Me	H	OMe	C-CH=NOH	H	50	≈20	5.6	0.76	0.37	1.0	-10.47 (E) (1//5) -9.84 (Z) (3//9)
22	Me	H	OMe	C-CH=NOH	H	50	≈20	1.0	2.1	0.33	0.97	
23	Me	OMe	H	C-CN	H	100[a]	0.3	0.00035	0.0002	0.00013	0.002	-10.78 (1//48)

	R_N	X	Y	Z	R_2	%TPI (at 20 μM)[a]	TPI IC_{50} [b]	HL-60 (10^{-6} M) [c]	A-549 (10^{-6} M)[c]	HeLa (10^{-6} M)[c]	HT-29 (10^{-6} M)[c]	Binding E (Cluster number // % of conf) [d]
24	Me	H	OMe	C-CN	H	87	>5	0.21	0.7	0.13	0.41	-10.10 (2//6)
25	Me	OMe	H	C-COOH	H	95	1.4	0.0072	0.087	0.033	0.065	-9.73 (1//53)
26	Me	H	OMe	C-COOH	H	7	>20	3.1	3.0	3.9	2.9	-9.17 (2//24)
27	Me	OMe	H	C-COOMe	H	95	0.7	0.0062	0.041	0.0073	0.022	-10.16 (1//19)
29	Me	OMe	H	C-CON(Me) $(CH_2)_2COOMe$		95	>20	0.305	0.159	1.6	0.235	
30	Me	OMe	H	C-CONH $(CH_2)_2COOEt$		100	3.0					
31	Me	OMe	H	C-CON(Me) $CH_2(COOMe)_2$		15[f]		0.239	0.156	1.17	0.306	
33	Me	OMe	H	C-CON(Me) CH_2COOH		38	>20	0.266	0.112	0.185	0.21	-6.23 (11//3)
34	Me	OMe	H	C-CONH $(CH_2)_2COOH$		92	13	0.404	>1	1.42	1.47	
35Z	Me	OMe	H	C-Br	H	100[a]	2.5	0.0368	0.442	0.309	0.346	
36Z	Me	OMe	H	C-Br	Br	100[a]	1.1	0.165	0.194	0.695	0.191	-10.07 (2//47)
37/38	Me	OMe	H	N	H	93	2.2	0.032	0.034	0.031	0.032	-9.40 (1//100)
37/38	-	OMe	H	NMe	H	49	≈20	0.03	0.22	0.028	0.029	-9.13 (1//96)

[a] Percentage tubulin polymerization inhibitory (TPI) activity at the indicated concentration. [b] Tubulin polymerization inhibitory (TPI) IC_{50}. [c] Values are derived from concentration-response curves using the XTT assay as described in the Experimental Section. Data are shown as the mean values of three experiments performed in triplicate. [d] AutoDock Binding Energies in kcal/mol for the best pose of the cluster with number representing the indicated number of poses out of a total of 100. [e] At 5μM. [f] At 10μM.

For all the pairs differing only in the disposition of the methoxy groups of ring A (e.g., compare the matched couples **15**/**16Z**, **17**/**18**, **19**/**20**, **21**/**22**, **23**/**24** and **25**/**26**), the compounds with a 2,3,4-trimethoxyphenyl (like that of colchicine) were less potent than those with a 3,4,5-trimethoxyphenyl

ring (like those of podophyllotoxin and combretastatin A4), similar to what has been reported previously.[22] Comparison of **13** and **14** with **15** and **17** respectively, shows that a methyl is slightly preferred over an ethyl on the indole nitrogen.

Substitutions at the indole 3 position (e.g. **17**, **19**, **21**, **23** and **25**) result in an overall potency increase with respect to the unsubstituted **15** for the 3,4,5-trimethoxyphenyl substituted compounds whereas an opposite trend is seen for compounds with a 2,3,4-trimethoxyphenyl (e.g., compare **18**, **20**, **22**, **24** and **26** with **16Z**). This different behavior probably arises from steric hindrance, as larger groups result in more reduced potencies, in agreement with previous results on the isocombretastatins where indole substitution causes a reduction in potency.[13] We have previously shown that substituents protruding out of the plane of ring B in isocombretastatins result in less potent compounds.[23]

The optimal substitutions at the indole 3 position are the hydroxyiminomethyl (**21**) and the cyano (**23**) groups, which are nanomolar or subnanomolar in the four cell lines assayed. The formyl substituent (**17**) provides also high potency against HeLa and HL60, but there is a significant potency drop down to the micromolar range for A549 and HT-29. For the second potency level (two digit nanomolar), carboxy (**25**), methoxycarbonyl (**27**) and hydroxymethyl (**19**) indoles and the *N*-methylbenzimidazoles (**37**, **38**) show similar potencies in the four cell lines. Larger substitutions at the three position (**29**, **34**) result in a significant potency reduction, although most of them are still in the submicromolar range.

The effect of the compounds on in vitro bovine brain tubulin assembly was studied at concentrations between 5 and 20 μM (Table 2). For those compounds inhibiting tubulin polymerization more than 50% at 20 μM we determined the IC_{50} values of tubulin polymerization inhibition (TPI). These values allowed us to compare the potencies of different compounds and to analyze the relationship between structure and TPI. Most of the compounds showed potent TPI inhibitory activity with values below 20 μM, many better than combretastatin A4 (IC_{50} = 3 μM). As seen for the cytotoxicity assays, the 3,4,5-

trimethoxyphenyl and 3 substituted *N*-methylindole combination was optimal, with several compounds (e.g. **17**, **21**, **23** and **27**) showing submicromolar values. The compounds with a 2,3,4-trimethoxyphenyl ring showed reduced potencies, typically a ten - fold reduction as for example from **19** to **20**. Substitution of the indole *N*-methyl by an *N*-ethyl modestly reduces the TPI potency. The TPI results show that aldehyde (**17**), hydroxyiminomethyl (**21**), nitrile (**23**), and methoxycarbonyl (**27**) substituents at the 3-position of the indole are optimal for tubulin inhibition. These groups share a sp2 carbonyl or equivalent conjugated with the indole ring and both hydrogen-bond donors and acceptors are allowed. Comparison of the TPI and cytotoxicity IC_{50} values shows that there is a good overall agreement between the TPI and the cytotoxic potencies against HeLa and HL60 cells, while the effects against A-549 and HT-29 show in some cases significant deviations. These results suggest either a difference in the target (different tubulin isotype expression) or the involvement of an additional effect (drug efflux, drug metabolism, or other) to account for the observed potency reduction in these cell lines.

Figure 2. Effects of compounds **17**, **21** and **23** on the microtubule network of Hela cells. Cells were incubated in the absence (Control) or in the presence of 10 or 100 nM of compounds **17**, **21** and **23** for 15 h and then fixed and processed to analyze microtubules (red fluorescence) and nuclei (blue fluorescence) as described in the Experimental Section. Bar: 25 μm. The photomicrographs shown are representative of at least three independent experiments performed.

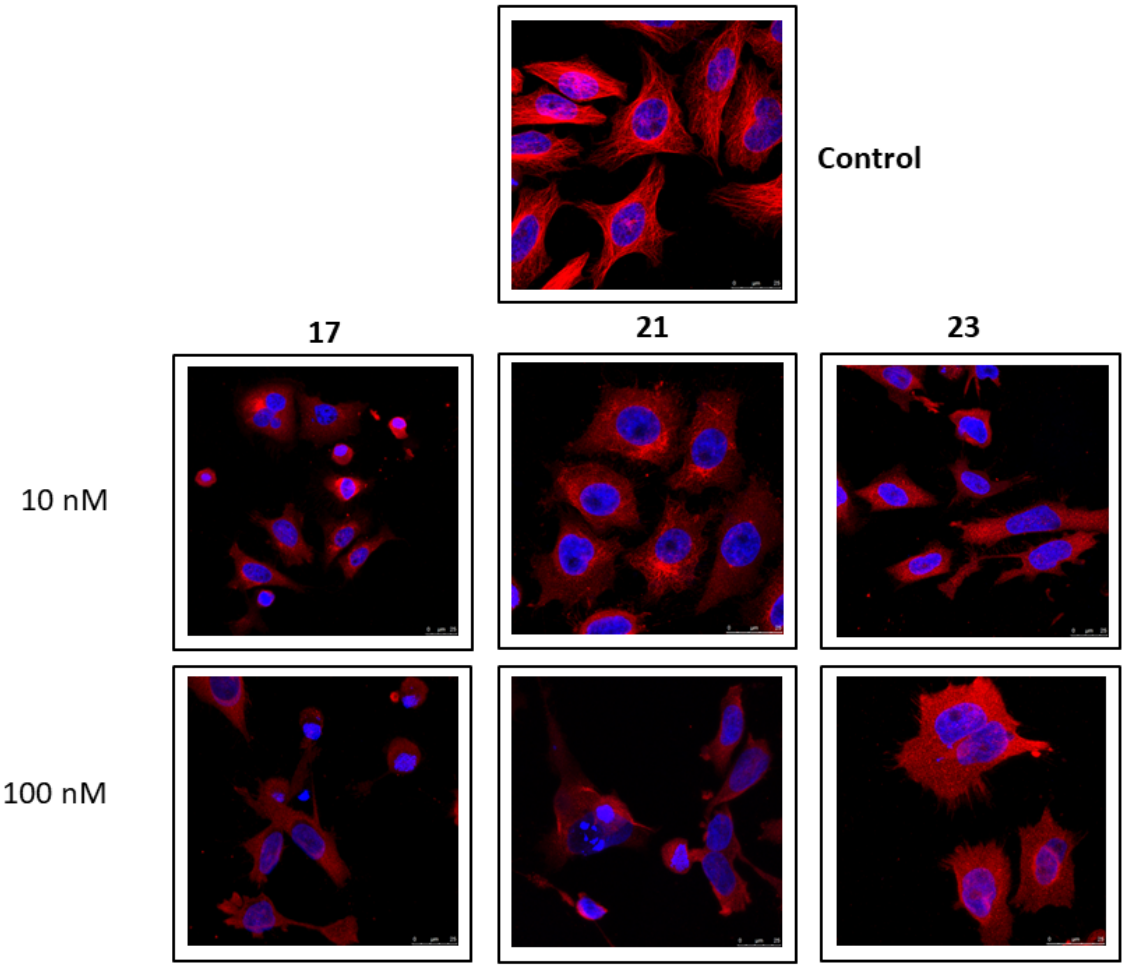

The three compounds that showed a lower IC_{50}, namely **17**, **21** and **23**, led to a drastic and severe disruption of the microtubule network of HeLa cells at nanomolar concentrations (Figure 2), further confirming that the observed effects were due to interaction with tubulin. Dose-response and time-course analyses of the most active compounds synthesized in this work (**16E**, **17**, **21**, **23**, **25**, **27**, **30**) showed a major cell cycle arrest at G_2/M phase (Figure 3), followed by the induction of apoptotic cell death, as assessed by an increase in the percentage of cells at the sub-G_0/G_1 region, representing cells undergoing chromosomal DNA degradation (Supplementary Table S1).

Figure 3. Effect of different compounds on the distinct cell cycle phases in HeLa cells. Compounds **16E**, **17**, **21**, **23**, **25**, **27** and **30** were incubated for 15 h and then their DNA content was analyzed by flow cytometry as described in the Experimental Section. The different cell cycle phases were

quantified and represented in pie charts to easily visualize the changes in G_2/M arrest. Untreated control cells were run in parallel. Data shown are representative of at least three independent experiments performed.

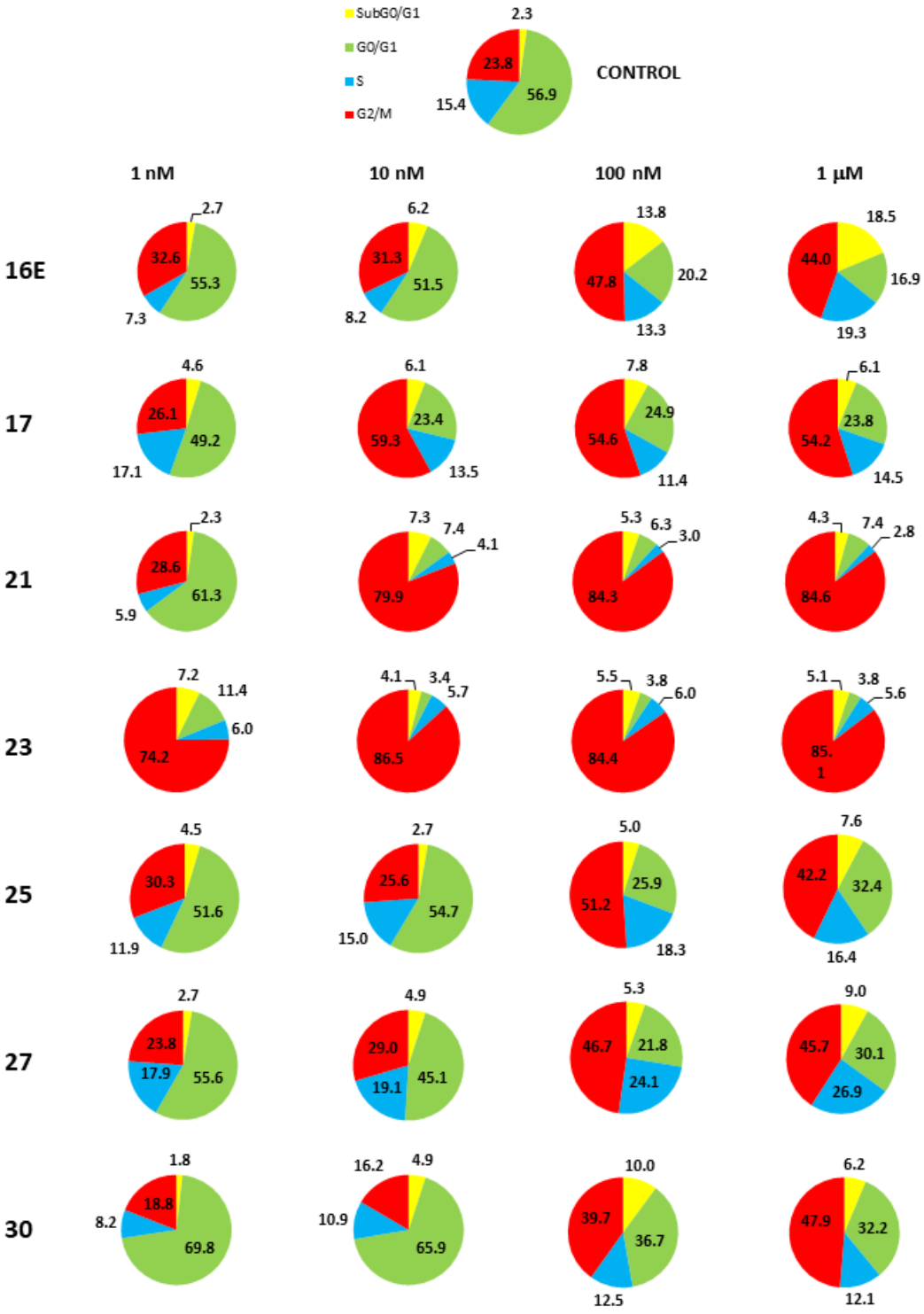

Compound **23** was the most active one in arresting most of the cells (74.2%) at the G2/M phase at only 1 nM concentration and after 15 h incubation, followed by compound **21** (79.9%) and **17** (59.3%), which required 10 nM concentration (Supplementary Table S1, and Figure 3).

Figure 4. Time-course of the effects of compounds **21** and **23** on cell cycle in HeLa cells. Cells were incubated with 1 or 10 nM of **21** and **23** for the indicated times, and their DNA content was analyzed by fluorescence flow cytometry. The positions of the G_0/G1 and G_2/M peaks are indicated by arrows, and the proportion of cells in each phase of the cell cycle was quantified by flow cytometry. The cell population in the sub-G_0/G1 region represents cells with hypodiploidal DNA, an indicator of apoptosis, and the percentages of cells at this region are indicated in each histogram. Untreated control cells were run in parallel. The experiments shown were representative of three performed.

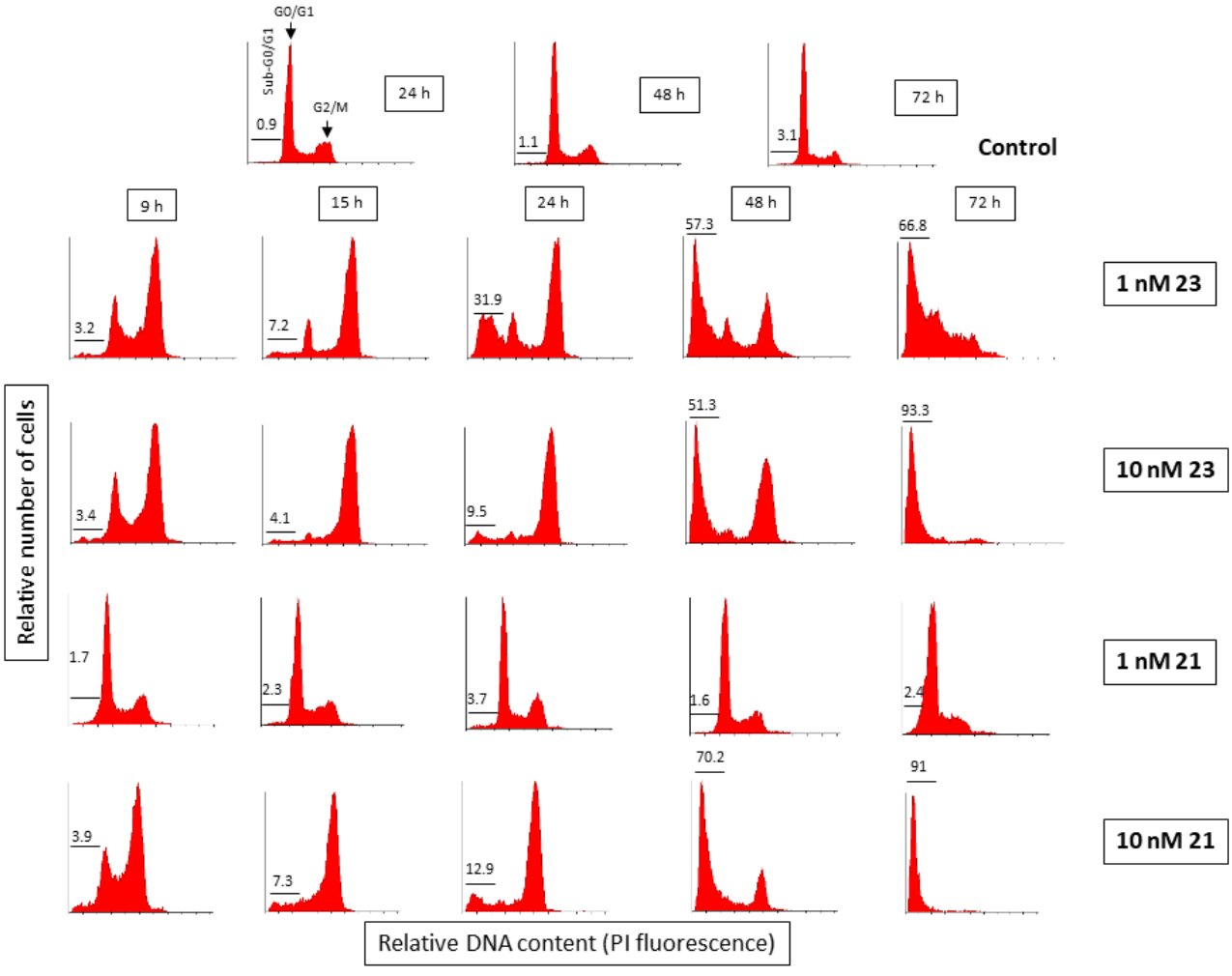

Figure 4 shows a time-course of the effects of the most active analogs **23** (active at 1 nM) and **21** (active at 10 nM) on the cell cycle profile of HeLa cells. G_2/M cell cycle arrest was evident even at only 9 h treatment, and the onset of apoptosis took place after 24 h incubation, and the cell death response was almost complete after 72 h treatment (Figure 4). Taken together, these data indicate that the actions of **23** and **21** on microtubules lead to a total disruption of microtubules that triggers a potent apoptotic response, rendering a complete cell demise in the drug-treated population. Caspase-3 activation was observed following treatment of HeLa cells with **23**, as assessed by the processing of procaspase-3 into the p17/p19 active form, and the cleavage of the typical caspase-3 substrate PARP into the 89-kDa cleaved form (Supplementary Figure S1). Interestingly, the combined incubation of **21** or **23** and 10 μM verapamil, a concentration that had been previously reported not to decrease cell viability,[24, 25] highly potentiated the cytotoxic activity of both **21** and **23** to IC_{50} of 10^{-10} M in A549 cells (Figure 5). Furthermore, the compound **17** became very active against A549 cells (IC_{50} = 5.98 x 10^{-8} M) when combined with 10 μM verapamil. These data suggest that the P-glycoprotein and calcium antagonist verapamil highly potentiate the cytotoxicity rendered by these newly synthetized combretastatin A-4 derivatives.

Figure 5. Effect of verapamil on the sensitivities of A549 cancer cells to **21** and **23**. Cells were co-incubated with verapamil and different concentrations of **21** and **23**. The dose–response curves were drawn using the GraphPad Prism 5 software. Results are mean values ± S.D. of a representative experiment carried out in triplicate, out of three performed.

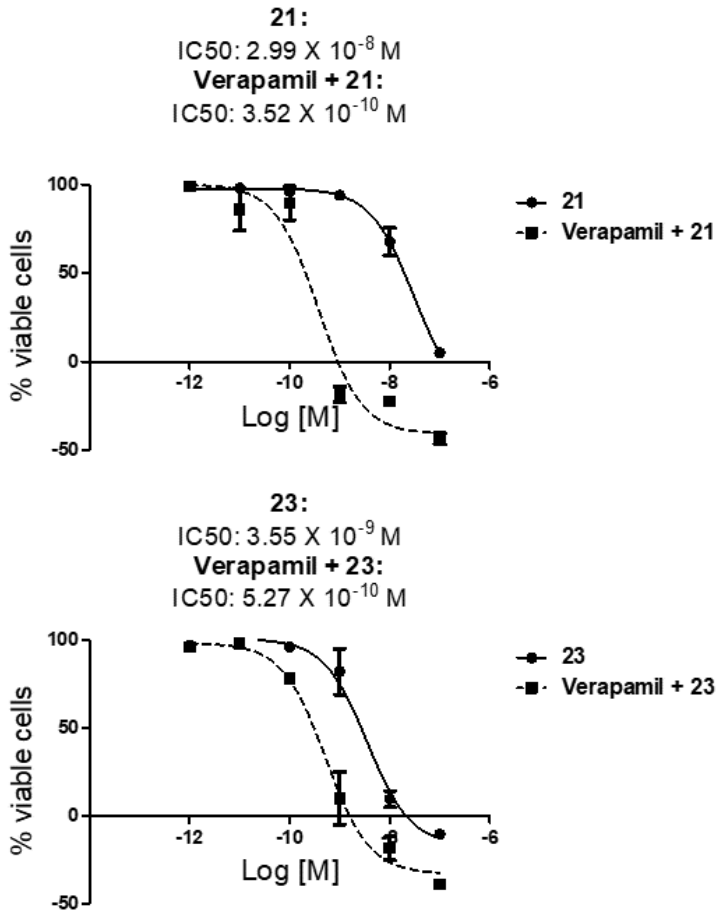

The different effect of the 3-substituents on the indole ring of isomeric combretastatins and isocombretastatins on their potency could be explained by their topological differences. Therefore, the preferred conformations of the compounds were calculated, DFT-optimized and those conformations better superimposing onto the X-ray crystal structure of combretastatin A-4 when in complex with tubulin (pdb ID 1LYJ)[26] were selected as the putative conformations binding to the colchicine site of tubulin. Figure XRAY shows the superimposition of the unsubstituted (a, **15**) and 3-cyano indole combretastatins (b, **23** with a 3,4,5-trimethoxyphenyl ring and c, **23** with a 2,3,4-trimethoxyphenyl ring) and isocombretastatins (d and e) onto combretastatin A4 (carbon atoms colored in cyan). All of them place the phenyl rings close to those of combretastatin A4 to comply with the essential role assigned by pharmacophoric models for ligands of the colchicine site to their spatial arrangement. The single atom sp2 hybridized connection between the phenyl rings of isocombretastatins results in a wider opening

angle between the ring centroids and the bridge than in a stilbene (Fig d and e). When in complex with tubulin this disposition of the rings either projects the 3 substituents at positions further away probably colliding with the site walls or forces the displacement of the trimethoxyphenyl ring in the opposite direction towards the site walls thus resulting in the observed potency reduction. Similarly, a 2,3,4-trimethoxyphenyl ring is more sterically demanding (Fig c) in the plane of the B – ring and trying to accommodate it in the colchicine site pushes the indole ring in the opposite sense. Substituents at the indole 3-position further worsen the steric problem and explains the potency decrease proportional to substituent size.

Figure 6. Best superpositions of the X-ray structure of combretastatin A4 (in cyan) in the complex with tubulin and the conformations of representative compounds showing the effects of the structural modifications and the corresponding docking results (the protein is shown in grey): a) with **15**; b) with **23**; c) with **24**; d) with the 11,diarylethene isomer (isocombretastatin) of **15** and e) with the 11,diarylethene isomer (isocombretastatin) of **24** and f) a combination of b,c and e.

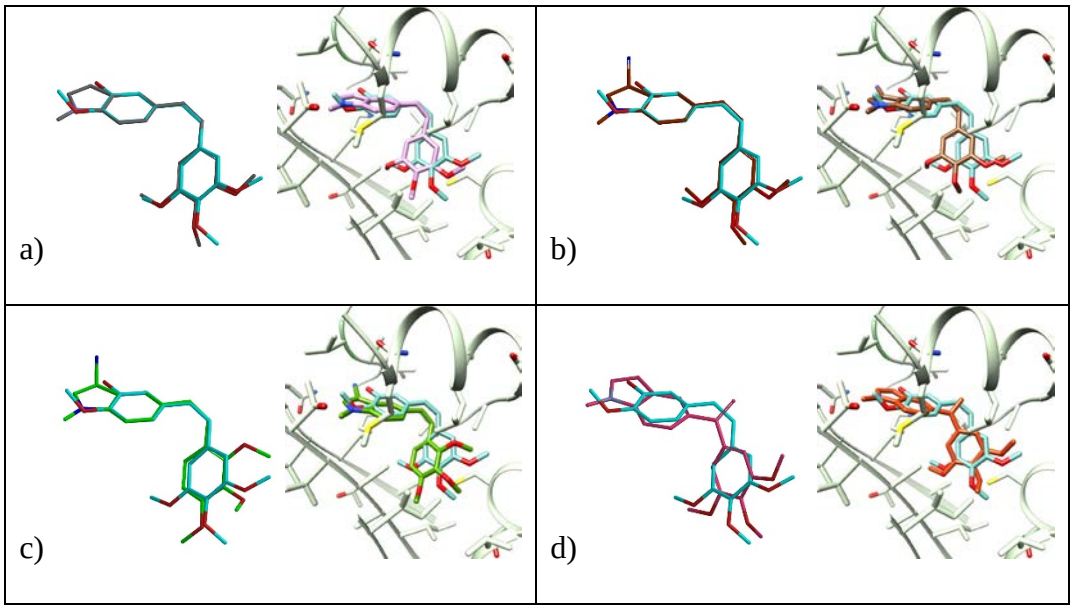

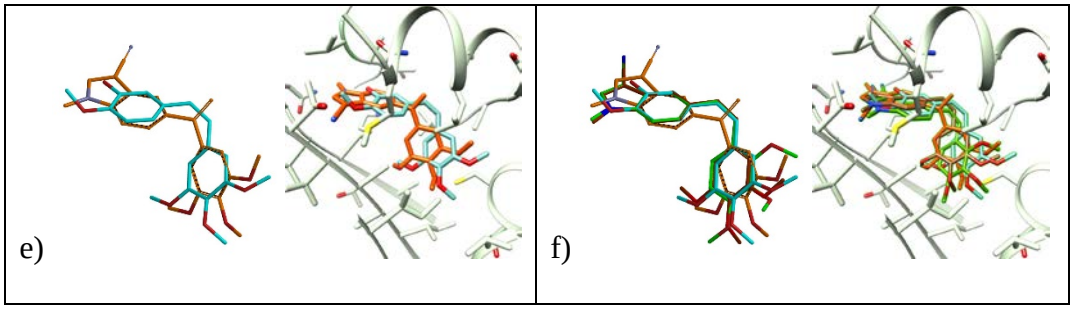

Docking experiments using AutoDock 4.2 on the X-ray structure of tubulin in complex with combretastatin A4 (pdb ID: 5LYJ) yielded results in excellent agreement with the experimental TPI and cytotoxicity results (Table 2) and with the results of the conformational study. When other X-ray structures of tubulin (15 different structures obtained from X-ray crystal structures of tubulin in complex with less structurally related ligands of the colchicine site or structures derived from molecular dynamics simulations, as previously described[13]) yielded worse results. The docking binding energy differences between compounds with a 3,4,5-trimethoxyphenyl (**15**, **17**, **19**, **21**, **23**, and **25**) and their matched pairs with a 2,3,4-trimethoxyphenyl ring (**16**, **18**, **20**, **22**, **24**, and **26**, respectively) is ca 0.6 kcal/mol, in good agreement with the differences observed for TPI IC_{50} values. Also, for the former group the lowest energy clusters correspond to the same ring dispositions as seen for combretastatin A4, whereas for the second group the clusters with this ring disposition are usually second or worse by energy, being usually surpassed by dispositions with the two phenyl rings switched. For the most potent analogues (**15**, **17**, **19**, **21**, **23**, **25** and **27**) the rank order of binding energies (**21**, **23, 19**, **17**, **27**, **15**, **25**, **19, CA-4**) roughly matches the TPI values (**23, 21**, **17**, **27**, **19**, **25**, **15, CA-4**), in spite of the fact that the energy differences between them are probably too small to be safely trusted. For the extended amides (**29**-**34**) the results are similar to those described for the 2,3,4-trimethoxyphenyl rings.

CONCLUSIONS

The replacement of the B ring of combretastatin A4 by 3 substituted indoles results in highly potent tubulin inhibition and cytotoxicity against several human cancer cell lines. This effect of the indole 3

substituents is highly context dependent, as it has been shown to be detrimental in the isomeric isocombretastatins or in compounds with a 2,3,4-trimethoxyphenyl ring. The optimal substituents are the cyano and hydroximinomethyl groups, whose compounds display high potency in all the studied cell lines, whereas compounds with other substituents show different potencies in different cell lines. Co-treatment with verapamil restores high potency in these later compounds, thus suggesting a resistance based on MDR efflux proteins. The lower effect observed of the co-treatment for the former compounds suggest a lower sensitivity to MDR efflux. The more potent compounds displayed low nanomolar cytotoxicity against several human cancer cell lines due to tubulin inhibition, complete G_2/M cell cycle arrest after 15 h followed by a high apoptosis-like cell response after 48-72 h mediated by caspase-3 activation. Molecular modeling studies support binding at the colchicine site and provide an explanation for the aforementioned SAR. These compounds are highly potent against cell lines intrinsically resistant to combretastatin A4 and therefore could reduce treatment resistance.

EXPERIMENTAL SECTION

Chemical synthesis

1-Methyl-1*H*-indole-5-carbaldehyde (1) and 1-Ethyl-1*H*-indole-5-carbaldehyde (1)

1.04 g (26 mmol) of NaOH and 20 mg of *n*-$Bu_4N^+HSO_4^-$ were added to a stirred solution of 1*H*-indole-5-carbaldehyde (2.0 g, 13,8 mmol) in 40 mL of dry CH_2Cl_2. After 1 hour at atmosphere temperature 3 mL (40.2 mmol) of methyl iodide or ethyl bromide were added and the reaction was heated at 50ºC. After 3 days the reaction mixture was concentrated, re-dissolved in CH_2Cl_2, washed with brine, dried over anhydrous Na_2SO_4, filtered and concentrated in vacuum to obtain 1,10 g (61%) of **1** and 1.48 g (62.0%) of **2**.

1-Ethyl-1*H*-indole-5-carbaldehyde (**1**): M.p.: 64-66 ºC (CH_2Cl_2/Hex). IR (KBr): 1703, 1605, 1307, 769 cm^{-1}. ^1H NMR (200 MHz, $CDCl_3$): δ 1.49 (3H, t, *J* = 7.2), 4.22 (2H, m), 6.66 (1H, d, *J* = 3.3); 7.22

(1H, d, *J* = 3.3), 7.42 (1H, d, *J* = 8.4), 7.78 (1H, dd, *J* = 8.4 and 1.4), 8.15 (1H, d, *J* = 1.4), 10.0 (1H, s). ^{13}C NMR (50 MHz, $CDCl_3$): δ 15.4 (CH_3), 41.2 (CH_2), 103.4 (CH), 109.9 (CH), 121.6(CH), 126.5 (CH), 128.4 (C), 128.5 (CH), 129.3 (C), 139.0 (C), 192.5 (CH).

1-Methyl-1*H*-indole-5-carbaldehyde (**2**): M.p.: 85-86ºC (Ether). ^{1}H NMR (200 MHz, $CDCl_3$): δ 3.76 (3H, s), 3.76 (3H, s) 6.55 (1H, d, *J* = 3.3), 7.10 (1H, d *J* = 3.3), 7.41(1H, d, *J* = 8.8), 7.80 (1H, dd, *J*= 8.8 and 1.9), 8.05 (1H, d, *J* = 1.9), 9.92 (1H, s). ^{13}C NMR (50 MHz, $CDCl_3$): δ 32.6 (CH_3), 103.1 (CH), 109.8 (CH),121.4 (CH), 126.1 (CH), 128.2(C), 129.1 (C), 130.9 (CH), 139.8 (C), 192.3 (CH).

1-Ethyl-1*H*-indole-3,5-dicarbaldehyde (3): IR (film): 1687, 1662, 1191 cm^{-1}. ^{1}H NMR (200 MHz, $CDCl_3$): δ 1.54 (3H, t, *J* = 7.2), 4.25 (2H, c, *J* = 7.2),7.44 (1H, d, *J* = 8.6), 7.84 (1H, s), 7.85 (1H, dd, *J* = 8.6 and 1.6), 8.73 (1H, d, *J* = 1.6), 9.99 (1H, s), 10.04 (1H, s). ^{13}C NMR (50 MHz, $CDCl_3$): δ 15.0 (CH_3), 42.1 (CH_2), 110.8 (CH), 118.8 (C), 123.4 (CH),125.0 (C), 126.8 (CH), 131.7 (C), 139.7 (CH), 140.1 (C), 184.5 (CH), 192.1 (CH).

3-Bromo-1-methyl-1*H*-indole-5-carbaldehyde (4) and 2,3-Bibromo-1-methyl-1*H*-indole-5-carbaldehyde (5)

To a solution of 1-methyl-1*H*-indole-5-carbaldehyde (2.0 g, 12.58 mmol) in 4 mL of chloroform, 2.9 g (16.35 mmol) of *N*-bromosuccinimide were slowly added. After 24 h stirring at 0 ºC, the reaction mixture was evaporated to obtain 5.38 g of crude. After column chromatography on silica gel (Hex/EtOAc 7/3) 611mg (1.93mmol, 15.34%) of compound **5** and 540 mg (2.27 mmol, 18.04%) of compound **4** were obtained.

3-Bromo-1-methyl-1*H*-indole-5-carbaldehyde (4): IR ^{1}H NMR (200 MHz, $CDCl_3$): δ 3.84 (3H, s), 7.26 (1H, s), 7.40 (1H, d, *J* = 8.8), 7.84 (1H, dd, *J* = 8.8 and 1.9), 8.09 (1H, d, *J* = 1.9), 10.07 (1H, s). ^{13}C NMR (50 MHz, $CDCl_3$): δ 33.3 (CH_3), 91.7 (C), 110.2 (CH), 122.4 (CH), 124.9 (CH), 127.3 (C), 129.5 (CH), 129.8 (C), 139.4 (C), 192.0 (CHO).

2,3-Dibromo-1-methyl-1*H*-indole-5-carbaldehyde (5): IR ^{1}H NMR (200 MHz, $CDCl_3$): δ 3.84 (3H, s), 7,40 (1H, d, *J* = 8.4), 7,85 (1H, dd, *J* = 1,0 and 7.4), 8.05 (1H, d, *J* = 0.8), 10.06 (1H, s). ^{13}C NMR (50 MHz, $CDCl_3$): δ 32.7 (CH_3), 94.9 (C), 100.2 (C), 110.3 (CH), 117.0 (C), 118.4 (C), 122.8 (CH), 126.9 (CH), 130.3 (C), 191.8 (CHO).

Preparation of compounds 7-10

To a suspension of 2,0 g (12.3 mmol) of 1*H*-benzo[*d*]imidazole-5-carboxylic acid in 50 mL of dry THF, in inert atmosphere was added 983 mg (24,7 mmol) of $LiAlH_4$ and stirred 48 h at 65ºC. The reaction mixture was poured into EtOAc/ EtOH and was filtered, by evaporation to dryness 1,4 g (75%) of compound 7 was obtained.

4.94 g (56.7 mmol) of MnO_2 were added to a solution of 1.40 g (9.46 mmol) of **7** in 50 mL of MeOH. After 48 h at rt, the mixture was filtered over sílica and by evaporation 1.24 g (90%) of compound **8** was isolated.

To a solution of 1.24 g (8.49 mmol) of **8** in 50 mL of CH_2Cl_2:H_2O (3:2) was added 700 mg (17.5 mmol) of NaOH and and 40 mg of *n*-$Bu_4N^+HSO_4$. After 1 h stirring 1.33 mL (21.2 mmol) of MeI were added. After 24 h After 3 days the reaction mixture was concentrated, re-dissolved in CH_2Cl_2. After chromatography on silica gel (CH_2Cl_2/EtOAc 85/15), 600 mg (44%) of a mixture **9** and **10** were obtained

1*H*-benzo[*d*]imidazol-5-yl)methanol (7): ^{1}H NMR (200 MHz, $CDCl_3$): δ 4.60 (2H, s), 7.08 (1H, dd; *J* = 8.4 and 1.6); 7,45 (1H, d, *J* = 8.4), 7.49 (1H, bs), 7.94 (1H, s). ^{13}C NMR (50 MHz, $CDCl_3$): δ 65.9, (CH_2), 115.2 (CH), 116.3 (CH), 121.3 (CH), 136.1 (C), 140.6 (C), 141.0 (C), 146.0 (CH).

1*H*-Benzo[*d*]imidazole-5-carbaldehyde (8): ^{1}H NMR (200 MHz, $CDCl_3$): δ 7.55 (1H, d, *J* = 8.4), 7.65 (1H, dd, *J* = 8,4 and 1.4), 8.01 (1H, bs), 8.24 (1H, s), 9.85 (1H, s). ^{13}C NMR (50 MHz, $CDCl_3$): δ 116.3 (CH), 120.5 (CH), 124.5 (CH), 133.1 (C), 139.7 (C), 142.8 (C), 145.9 (CH), 194.0 (CH).

1-Methyl-1*H*-benzo[d]imidazole-6-carbaldehyde(9) and 1-Methyl-1*H*-benzo[*d*]imidazole-5-carbaldehyde (10): ^{1}H NMR (200 MHz, $CDCl_3$): δ 3.60 (3H, s); 3.63 (3H, s), 7.17 (1H, d, *J* = 8.4), 7,56 (1H, dd, *J* = 8.4 and 1.6),7.56 (1H, dd, *J* = 8.4 and 1.6), 7.59 (1H, d, *J* = 8.4), 7.61 (1H, s), 7.77 (1H, s), 7.82 (1H, d, *J* = 1.6), 7.98 (1H, d, *J* = 1.6), 9.78 (1H, s), 9.79 (1H, s). ^{13}C NMR (50 MHz, $CDCl_3$): δ 31.2 (2) (CH_3), 110.1 (CH), 111.8 (CH), 120.2 (CH), 123.2 (CH), 123.5 (CH), 123.8 (CH), 131.3 (C), 131.5 (C), 134.5 (C), 138.7 (C); 143.4 (C), 145.9 (CH), 147.0 (CH), 148.1 (C), 191.7 (CH), 191.9 (CH).

(Z)-1-Ethyl-5-(3,4,5-trimethoxystyryl)-1*H*-indole (13)

To a suspension of triphenyl(3,4,5-trimethoxybenzyl)phosphonium bromide (1.67 g, 3.19 mmol) in dry THF (40 mL), at -40 ºC in argon atmosphere, *n*BuLi (1.6 M in hexane, 2.0 mL, 3.2 mmol) was added and stirred for 1 h. A solution of 1-ethyl-1*H*-indole-5-carbaldehyde (500 mg, 2.89 mmol) in dry THF (10 mL) was slowly added at -40 ºC and progressively warmed to room temperature. After 24 h, the reaction mixture was poured into ammonium chloride solution and extracted with CH_2Cl_2. The organic layers were washed to neutrality with brine, dried over anhydrous Na_2SO_4, filtered and evaporated to dryness. After chromatography on silica gel (Hex/AcOEt 85/15), 130 mg (0.40 mmol, 14%) of **13*Z*** and 161 mg (0.51 mmol, 18%) of a mixture **13*Z*/13*E*** were obtained.

(Z)-1-Ethyl-5-(3,4,5-trimethoxystyryl)-1*H*-indole (13): IR (film): 1685, 1579, 1127, 1007, 796, 722 cm^{-1}. ^{1}H NMR (200 MHz, $CDCl_3$): δ 1.51 (3H, t, *J* = 7.3), 3.62 (6H, s), 3.85 (3H, s), 4.18 (2H, c, *J* = 7.3), 6.41 (1H, d, *J* = 3.1); 6.43 (1H, d, *J* = 12.3), 6.57 (2H, s), 6.72 (1H, d, *J* = 12.3), 7.08 (1H, d, *J* = 3.1), 7.20 (1H, bs), 7.26 (1H, dd), 7.60 (1H, bs). ^{13}C NMR (50 MHz, $CDCl_3$): δ 15.5 (CH_3), 41.1 (CH_2), 55.9 (2) (CH_3), 60.9 (CH_3), 103.3 (CH), 106.1 (CH), 108.9 (CH), 121.7 (CH), 122.8 (CH), 127.4 (CH), 128.3 (C), 128.7 (C), 129.8 (CH), 131.4 (CH), 133.3 (C), 135.0 (C), 135.6 (C), 152.8 (2) (C). HRMS ($C_{21}H_{23}NO_3$): calcd. 337.1678 (M^+), found falta. HPLC

(*Z*)-1-Ethyl-5-(3,4,5-trimethoxystyryl)-1*H*-indole-3-carbaldehyde (14)

To a suspension of triphenyl(3,4,5-trimethoxybenzyl)phosphonium bromide (466 mg, 0.89 mmol) in dry THF (20 mL), at -40ºC in argon atmosphere, *n*BuLi (1.6 M in hexane, 0.56 mL, 0.89 mmol) was added and stirred for 1 h. The mixture was slowly added to a solution of 1-ethyl-1*H*-indole-3,5-dicarbaldehyde (189 mg, 0.89 mmol) in dry THF (10 mL) at -40 ºC and progressively warmed to room temperature. After 24 h, the reaction mixture was poured into ammonium chloride solution and extracted with CH_2Cl_2. The organic layers were washed to neutrality with saturated NaCl, dried over anhydrous Na_2SO_4, filetred and evaporated to dryness. By repeated chromatography with Hex/AcOEt 7/3 and CH_2Cl_2/AcOEt 96/4, aldehyde **14** (27 mg, 5.1%) was obtained. IR (film): 1655, 1459, 1397, 1124, 784 cm^{-1}. ^1H NMR (400 MHz, $CDCl_3$): δ 1.51 (3H, t, *J* = 7.2), 3.61 (6H, s), 3.82 (3H, s), 4.19 (2H, c, *J* = 7.2), 6.51 (1H, d, *J* = 12.2), 6.50 (2H, s), 6.73 (1H, d, *J* = 12.2), 7.19 (1H, d, *J* = 8.8), 7.30 (1H, dd, *J* = 8.8 and 2.0), 7.72 (1H, s), 8.26 (1H, bs), 9.96 (1H, s). ^{13}C NMR (100 MHz, $CDCl_3$): δ 15.1 (CH_3), 42.0 (CH_2), 55.9 (2) (CH_3), 61.0 (CH_3), 106.2 (2) (CH), 109.4 (CH), 118.2 (C), 122.8 (CH), 125.2 (CH), 125.6 (C), 129.4 (CH), 130.4 (CH), 132.3 (C), 132.9 (C), 136.0 (C), 137.2 (C), 137.6 (CH), 152.8 (2) (C), 184.4 (CH). MS: 365 (M^+). HPLC: C_{18} t_R: 19.9 min.

(*Z*)-1-Methyl-5-(3,4,5-trimethoxystyryl)-1*H*-indole (15). Referencia 16c

(*Z*)-1-Methyl-5-(2,3,4-trimethoxystyryl)-1*H*-indole (16*Z*)

To a stirred suspension of 2,3,4-Trimethoxybenzyltriphenylphosphonium bromide (1. 8 g, 3.46 mmol) in dry THF (10 mL), BuLi (1.6 M in hexane, 2.4 mL, 3.80 mmol) was added at -40 ºC under argon. After 1 h, 1-methyl-1*H*-indole-5-carbaldehyde (500 mg, 3.14 mmol) was added and the mixture was allowed to reach room temperature. After 12 h, the reaction mixture was poured onto ice with ammonium chloride and extracted with CH_2Cl_2. The combined organic layers were dried over Na_2SO_4 and the solvent was evaporated in vacuo. The residue was purified by flash chromatography on silica with hexane/EtOAc (7:3) obtaining **16*Z*** (590 mg, 58%) and **16*E*** **(**112 mg, 11%).

(*Z*)-1-Methyl-5-(2,3,4-trimethoxystyryl)-1*H*-indole (16*Z*): IR: 1596, 1493, 730 cm^{-1}. ^{1}H NMR (400 MHz, $CDCl_3$): δ 3.75 (3H, s), 3.83 (3H, s), 3.94 (6H, s), 6.41 (1H, bs), 6.45 (1H, d, *J* = 7.9), 6.58 (1H, d, *J* = 12.2), 6.78 (1H, d, *J* = 12.2), 6.98 (1H, d, *J* = 7.9), 7.02 (1H, bs), 7.16 (2H, m), 7.56 (1H, bs). ^{13}C NMR (100 MHz, $CDCl_3$): δ 32.8 (CH_3), 56.0 (CH_3), 61.1 (CH_3), 61.2 (CH_3), 101,3 (CH), 107.1 (CH), 108.8 (CH), 121.5 (CH), 122.8 (CH), 123.0 (CH), 124.6 (CH), 124.9 (C), 128.4 (C), 128.7 (C), 129.1 (CH), 131.1 (CH), 135.9 (C), 142.2 (C), 152.1 (C), 152.7 (C). HRMS ($C_{20}H_{21}NO_3$ + Na): calcd 346.1413 (M^+ + Na), found 346.1401. HPLC: C_{18} t_R: 22.4 min.

(*E*)-1-Methyl-5-(2,3,4-trimethoxystyryl)-1*H*-indole (16*E*): Mp 110-111ºC (Hexane). IR: 1492, 850 cm^{-1}. ^{1}H NMR (400 MHz, $CDCl_3$): δ 3.78 (3H, s), 3.90 (3H, s), 3.94 (3H, s), 3.95 (3H, s), 6.51 (1H, d, *J* = 3.4), 6.73 (1H, d, *J* = 8.6), 7.04 (1H, d, *J* = 3.4), 7.19 (1H, d, *J* = 16.5), 7.31 (1H, d, *J* = 8.6), 7.35 (1H, d, *J* = 8.6), 7.37 (1H, d, *J* = 16.5), 7.52 (1H, dd, *J* = 8.6 and *J* = 1.8), 7.76 (1H, d, *J*=1.8). ^{13}C NMR (100 MHz, $CDCl_3$): δ 32.9 (CH_3), 56.1 (CH_3), 61.0 (CH_3), 61.4 (CH_3), 101.3 (CH), 107.9 (CH), 109.5 (CH), 119.5 (CH), 120.0 (CH), 120.2 (CH), 120.3 (CH), 120.4 (CH), 125.3 (C), 128.8 (C), 129.4 (CH), 129.6 (C), 136.5 (C), 142.2 (C), 151.5 (C), 152.8 (C). HRMS ($C_{20}H_{21}NO_3$ + Na): calcd 346.1413 (M^+ + Na), found 346.1401. HPLC: C_{18} t_R: 23.1 min.

(*Z*)-1-Methyl-5-(3,4,5-trimethoxystyryl)-1*H*-indole-3-carbaldehyde (17)

A solution of $POCl_3$ (0.12 mL, 1.3 mmol) in DMF (1.0 mL) was stirred at 0 ºC for 1 h and then (*Z*)-5-(3,4,5-trimethoxystyryl)-1-methyl-1*H*-indole (395 mg, 1.23 mmol) was added and heated at 60 ºC for 2 h. After that, the reaction mixture was poured onto ice with sodium acetate, water (100 mL) was added and the mixture was keeped at 4 ºC. After 24 h the obtained precipitate was re-dissolved in CH_2Cl_2, dried over anhydrous Na_2SO_4, filtered, and concentrated in vacuum to obtain (*Z*)-*N*-methyl-5-[2-(3,4,5-trimethoxyphenyl)vinyl]indole-3-carbaldehyde (**17**) (400 mg, 93%). M.p.: 144-146ºC. (CH_2Cl_2/Hex). IR (KBr): 1650, 1456, 1128 cm^{-1}. ^{1}H NMR (400 MHz, $CDCl_3$): δ 3.62 (6H, s), 3.84 (3H, s), 3.86 (3H, s),

6.52 (2H, s), 6.52 (1H, d, *J* = 12.4), 6.73 (1H, d, *J* = 12.4), 7.18 (1H, d, *J*=9.2), 7.32 (1H, dd, *J* = 9.2 and 2.2), 7.66 (1H, bs), 8.27 (1H, s), 9.98 (1H, s). ^{13}C NMR (100 MHz, $CDCl_3$): δ 33.5 (CH_3), 55.8 (2) (CH_3), 60.8 (CH_3), 106.2 (2) (CH), 109.6 (CH), 117.9 (C), 122.4 (CH), 125.1 (CH), 125.2 (C), 129.2 (CH), 130.3 (CH), 132.1 (C), 132.8 (C), 137.0 (C), 137.2 (C), 140.1 (CH), 152.8 (2) (C), 184.3 (CH). HRMS ($C_{21}H_{21}NO_4$ + Na): calcd 374.1368 (M^+ + Na), found 374.1343 HPLC: C_{18} t_R: 14.66 min. C_8 t_R: 13.42 min. Phenylic t_R: 14.24 min.

(*Z*)-1-Methyl-5-(2,3,4-trimethoxystyryl)-1*H*-indole-3-carbaldehyde (18)

$POCl_3$ (360 mg, 2.3 mmol) in dry DMF (1 mL) at 0ºC was stirred for 30 min, then compound **16*Z*** (720 mg, 2.2 mmol) was added and the reaction was heated at 60ºC for 2 h. The reaction mixture was poured onto ice with sodium acetate, after 24 h at 2ºC, the solid obtained was filtered, solved in CH_2Cl_2, dried over Na_2SO_4 and the solvent evaporated in vacuo. The residue was purified by flash chromatography on silica gel with hexane/EtOAc (8:2) aldehyde **18 (**661 mg, 85%). ^{1}H NMR (400 MHz, $CDCl_3$): δ 3.64 (3H, s), 3.70 (3H, s), 3.90 (6H, s), 6.41 (1H, d, *J* = 8.6), 6.62 (1H, d, *J* = 12.1), 6.24 (1H, d, *J* = 12.1), 6.84 (1H, d, *J* = 8.6), 7.11 (1H, d, *J* = 8.6), 7.20 (1H, d, *J* = 8.6), 7.51 (1H, s), 8.18 (1H, bs), 9.92 (1H, s). ^{13}C NMR (100 MHz, $CDCl_3$): δ 33.6 (CH_3), 55.9 (CH_3), 60.8 (CH_3), 61.0 (CH_3), 107.0 (CH), 109.3 (CH), 118.1 (C), 122.5 (CH), 124.1 (CH), 124.3 (CH), 124.3 (C), 124.4 (CH), 124.7 (C), 130.1 (CH), 132.5 (C), 136.8 (C), 139.2 (CH), 142.2 (C), 152.0 (C), 152.9 (C), 184.2 (CH). HRMS ($C_{21}H_{21}NO_4$ + Na): calcd. 374.1368 (M^+ + Na), found 374.1349. HPLC: C_{18} t_R: 19.7 min.

(*Z*)-(1-Methyl-5-(3,4,5-trimethoxystyryl)-1*H*-indol-3-yl)methanol (19)

$NaBH_4$ (20 mg, 0.07 mmol) was added to a stirred solution (*Z*)-*N*-methyl-5-[2-(3,4,5-trimethoxyphenyl)vinyl]indole-3-carbaldehyde (24.6 mg, 0.07 mmol) in MeOH (10 mL). After half an hour, the methanol was evaporated and the residue was re-dissolved in CH_2Cl_2 and washed with brine. The organic layers were dried over anhydrous Na_2SO_4, filtered, and evaporated under vacuum to give (*Z*)-[*N*-methyl-5-[2-(3,4,5-trimethoxyphenyl)vinyl]indol-3-yl]methanol (**19**) (22 mg, 89%). IR (film):

3413, 1579, 1124 cm^{-1}. ^{1}H NMR (400 MHz, $CDCl_3$): δ 3.64 (6H, s), 3.74 (3H, s), 3.84 (3H, s), 4.79 (2H, bs), 6.44 (1H, d, *J* = 12.2), 6.57 (2H, s), 6.71 (1H, d, *J* = 12.2), 7.02 (1H, s), 7.14 (1H, d, *J* = 8.6), 7.25 (1H, dd, *J* = 8.6 and 1.8), 7.67 (1H, d, *J* = 1.8). ^{13}C NMR (100 MHz, $CDCl_3$): δ 32.8 (CH_3), 56.0 (2) (CH_3), 57.0 (CH_2), 61.0 (CH_3), 106.1 (2) (CH), 109.0 (CH), 115.0 (C), 120.0 (CH), 123.4 (CH), 127.0 (C), 128.1 (2) (CH), 128.5 (C), 131.1 (CH), 133.3 (C), 136.6 (C), 137.0 (C), 152.9 (2) (C). HRMS. Calcd. for ($C_{21}H_{23}NO_4$ + Na): calcd 376.1325 (M^+ + Na), found 376.1525. HPLC: C_{18} t_R: 14.82 min. C_8 t_R: 13.50 min. Phenylic t_R: 13.96 min.

(*Z*)-(1-Methyl-5-(2,3,4-trimethoxystyryl)-1*H*-indol-3-yl)methanol (20)

To a solution of aldehyde **18** (78 mg, 0.22 mmol) in MeOH (10 mL) at 0ºC and under argon, an excess of $NaBH_4$ (62 mg) was added. After 15 min the MeOH was evaporated and the residue dissolved in CH_2Cl_2, the organic layer was washed with water, dried over Na_2SO_4 and the solvent evaporated in vacuo and by crystallization in MeOH, to produce alcohol **20** (40 mg, 50%) as a white solid. Mp: 135-136ºC ($CHCl_3$/ether). IR (KBr) 3424, 1600, 1490 cm^{-1}. ^{1}H NMR (400 MHz, $CDCl_3$): δ 3.69 (3H, s), 3.81 (3H, s), 3.93 (6H, s), 4.76 (2H, s), 6.42 (1H, d, *J* = 8.6), 6.56 (1H, d, *J* = 12.1), 6.72 (1H, d, *J* = 12.1), 6.93 (1H, d, *J* = 8.6), 6.98 (1H, s), 7.10(1H, d, *J* = 8.5), 7.16 (1H, d, *J* = 8.5), 7.60 (1H, s), 7.82 (1H, bs). ^{13}C NMR (100 MHz, $CDCl_3$): δ 32.6 (CH_3), 55.9 (CH_3), 56.8 (CH_2), 60.9 (CH_3), 61.0 (CH_3), 107.0 (CH), 108.9 (CH), 115.0 (C), 119.7 (CH), 123.0 (CH), 123.2 (CH), 124.4 (CH), 124.7 (C), 126.8 (C), 127.9 (CH), 128.7 (C), 130.8 (CH), 136.3 (C), 142.2 (C), 152.0 (C), 152.7 (C). HRMS. Calcd. for ($C_{21}H_{23}NO_4$ + Na): calcd 376.13519 (M^+ + Na), found 376.1512. HPLC: C_{18} t_R: 19.3 min.

(*Z*+*E*)-1-Methyl-5-(3,4,5-trimethoxystyryl)-1*H*-indole-3-carbaldehyde oxime (21*Z*+*E*)

To a solution of aldehyde **17** (500 mg, 1.42 mmol) in MeOH (30 mL) hydroxylamine hydrochloride (987 mg, 14.2 mmol) and two drops of pyridine were added. After 24 at reflux, the solvent was evaporated, the obtained residue was solved in CH_2Cl_2 and extracted with H_2O. The combined organic

layers were dried over Na_2SO_4 and evaporated to give a residue that was purified by silica gel flash chromatography using hexane/EtOAc (8:2) to yield the oximes **21** (280 mg, 73%) as a mixture (3:2) of *Z* and *E* isomers. ^{1}H NMR (400 MHz, $CDCl_3$): δ 3.62 (6H, s), 3.67 (6H, s), 3.75 (3H, s), 3.83 (3H, s), 3.84 (3H, s), 3.86 (3H, s), 6.50 (1H, d, *J* = 12.6), 6.51 (1H, d, *J* = 12.6), 6.53 (2H, s), 6.58 (2H, s), 6.68 (1H, d, *J* = 12.6), 6.73 (1H, d, *J* = 12.6), 7.13-7.40 (6H, m), 7.72 (1H, s), 7.73 (1H, s), 8.23 (1H, s), 8.24 (1H, s). ^{13}C NMR (100 MHz, $CDCl_3$): δ 33.0 (CH_3), 33.4 (CH_3), 55.8 (2) (CH_3), 55.9 (2) (CH_3), 60.9 (2) (CH_3), 106.0 (2) (CH), 106.1 (2) (CH), 108.8 (CH), 109.3 (CH), 109.1 (2) (C), 118.7 (CH), 122.7 (CH), 124.2 (CH), 124.8 (CH), 128.3 (CH), 128.9 (CH), 129.8 (C), 130.3 (C), 130.5 (CH), 130.5 (C), 131.0 (CH), 131.5 (CH), 132.9 (C), 133.5 (C), 135.2 (C), 135.9 (CH), 135.9 (C), 136.8 (C), 137.0 (C), 137.2 (C), 145.3 (2) (CH), 152.8 (2) (C), 153.0 (2) (C). HPLC: C_{18} t_R: 19.5 and 20.3 min.

(*Z*+*E*)-1-Methyl-5-(2,3,4-trimethoxystyryl)-1*H*-indole-3-carbaldehyde oxime (22*Z*+*E*): ^{1}H NMR (400 MHz, $CDCl_3$): δ 3.72 (3H,s), 3.77 (3H, s), 3.82 (6H, s), 3.92 (12H, s), 6.44 (1H, d, *J* = 8.8), 6.46 (1H, d, *J* = 8.8), 6.60 (1H, d, *J* = 12.1), 6.62 (1H, d, *J* = 12.1), 6.75 (1H, d, *J* = 12.1).6.88 (1H, d, *J* = 8.8), 6.91 (1H, d, *J* = 8.8), 7.15-7.35 (4H, m), 7.17 (1H, s), 7.26 (1H, s), 7.66 (1H,s), 7.68 (1H, s), 8.18 (1H, s), 8.26 (1H, s). ^{13}C NMR (100 MHz, $CDCl_3$): δ 33.1 (CH_3), 33.2 (CH_3), 55.9 (CH_3), 56.0 (CH_3), 60.9 (CH_3), 61.0 (CH_3), 105.5 (C), 107.1 (CH), 107.3 (CH), 109.0 (CH), 109.2 (C), 109.6 (CH), 118.6 (CH), 120.5 (C), 121.4 (C), 122.7 (CH), 123.6 (CH), 123.7 (CH), 123.8 (CH), 124.2 (CH), 124.3 (C), 124.4 (CH); 124.9 (CH), 125.2 (C), 125.5 (C), 127.2 (C), 130.2 (C), 130.3 (CH), 130.4 (CH), 130.9 (CH), 134.9 (C), 135.3 (CH), 136.6 (C), 139.5 (CH), 142.2 (C), 145.5 (CH), 151.9 (C), 152.0 (C), 152.7 (C), 152.8 (C).

HPLC: C_{18} t_R: 19.5 and 20.5 min.

(*Z*)-1-Methyl-5-(3,4,5-trimethoxystyryl)-1*H*-indole-3-carbonitrile (23) and (*Z*)-1-Methyl-5-(2,3,4-trimethoxystyryl)-1*H*-indole-3-carbonitrile (24)

To a mixture of (*Z*+*E*) oximes **21** (80 mg, 0.21 mmol) or **22** (250 mg, 0.65 mmol) dissolved in pyridine (0.4 mL) or (1.25 mL) acetic anhydride (0.4 mL) or (1.25 mL) was added. After 9 h at room temperature, the reaction was treated with HCl 2N, extracted with CH_2Cl_2, washed with NaOH 2%, dried over anhydrous Na_2SO_4 and the solvent evaporated. The residue was purified by flash chromatography with hexane/EtOAc (1:1) yielding compound **23** (30 mg, 41%) or **24** (35 mg, 16%).

(*Z*)-1-methyl-5-(3,4,5-trimethoxystyryl)-1*H*-indole-3-carbonitrile (23): IR (film): 2217, 1579, 1504 cm^{-1}. ^1H NMR (400 MHz, $CDCl_3$): δ 3.63 (3H, s), 3.83 (3H, s), 3.85 (6H, s), 6.50 (2H, s), 6.53 (1H, d, *J* = 12.2), 6.68 (1H, d, *J* = 12.2), 7.21 (1H, d, *J* = 8.6), 7.30 (1H, d, *J* = 8.6), 7.52 (1H, s), 7.69 (1H, s). ^{13}C NMR (100 MHz, $CDCl_3$): δ 33.6 (CH_3), 55.9 (2) (CH_3), 60.9 (CH_3), 85.6 (C), 106.1 (2) (CH), 109.8 (CH), 115.6 (C), 120.3 (CH), 125.1 (CH), 127.8 (C), 129.7 (2) (CH), 131.5 (C), 132.6 (C), 135.0 (C), 135.7 (CH), 137.3 (C), 152.9 (2) (C). HRMS ($C_{21}H_{20}N_2O_3$ + Na): calcd 371.1366 (M^+ + Na), found 371.1353. HPLC: C_{18} t_R: 20.9 min.

(*Z*)-1-Methyl-5-(2,3,4-trimethoxystyryl)-1*H*-indole-3-carbonitrile (24): IR: 2216, 1596, 1490 cm^{-1}. ^1H NMR (400 MHz, $CDCl_3$): δ 3.73 (3H, s), 3.90 (9H, s), 6.43 (1H, d, *J* = 8.6), 6.65 (1H, d, *J* = 12.1), 6.71 (1H, d, *J*= 12.1), 6.83 (1H, d, *J* = 8.6), 7.16 (1H, d, *J* = .8), 7.24 (1H, d, *J* = 8.6), 7.50 (1H, s), 7.63 (1H, s). ^{13}C NMR (100 MHz, $CDCl_3$): δ 33.5 (CH_3), 55.9 (CH_3), 60.8 (CH_3), 60.9 (CH_3), 85.6 (C), 107.1 (CH), 109.8 (CH), 115.6 (C), 120.1 (CH), 124.0 (C), 124.2 (CH), 124.8 (CH), 125.0 (CH), 127.8 (C), 129.1 (CH). 131.8 (C), 135.0 (C), 135.7 (CH), 142.3 (C), 152.0 (C), 153.0 (C). HPLC: C_{18} t_R: 20.5 min.

(*Z*)-1-Methyl-5-(3,4,5-trimethoxystyryl)-1*H*-indole-3-carboxylic acid (25) and (*Z*)-1-Methyl-5-(2,3,4-trimethoxystyryl)-1*H*-indole-3-carboxylic acid (26)

A solution of 80% $NaClO_2$ (1.03 g, 11.4 mmol) and $NaH_2PO_4 \cdot 2H_2O$ (1.02 g, 8.53 mmol) in water (15 mL) was added at 0ºC to a suspension of aldehyde **17** (200 mg, 0.57 mmol) or **18** (200 mg, 0.57 mmol) in *tert*-butyl alcohol (15 mL) and 2-methylbut-2-ene (15 mL). THF (5 mL) was added to dissolve starting aldehyde **17** or **18** and the mixture was stirred at room temperature for 12 h. After dilution with

water (30 mL), the product was extracted with CH_2Cl_2, washed with brine, dried over anhydroud Na_2SO_4 and evaporated. By crystallization in MeOH (*Z*)-1-methyl-5-(3,4,5-trimethoxystyryl)-1*H*-indole-3-carboxylic acid (**25**) (150 mg, 72%) or **26** (180 mg, 86%) were obtained.

(*Z*)-1-Methyl-5-(3,4,5-trimethoxystyryl)-1*H*-indole-3-carboxylic acid (25): M.p.: 164-165ºC (MeOH). IR (KBr): 3450, 1620, 1502 cm^{-1}. ^1H NMR (400 MHz, $CDCl_3$): δ 3.64 (6H, s), 3.82 (3H, s), 6.50 (1H, d, *J* = 12.1), 6.51 (2H, s), 8.76 (1H, d, *J* = 12.1), 7.18 (1H, d, *J* = 8.5), 7.28 (1H, d, *J* = 8.5), 7.83 (1H, s), 8.20 (1H, s). ^{13}C NMR (100 MHz, $CDCl_3$): δ 33.5 (CH_3), 55.8 (2) (CH_3), 60.8 (CH_3), 106.1 (2) (CH), 106.3 (C), 109.3 (CH), 122.4 (CH), 124.3 (CH), 126.8 (C), 128.9 (CH), 130.6 (CH), 131.4 (C), 132.9 (C), 136.4 (C), 136.5 (CH), 137.1 (C), 152.8 (2) (C), 169.8 (C). HRMS ($C_{21}H_{21}NO_5$ + Na): calcd. 390.1311 (M^+ + Na), found 390.1318. HPLC: C_{18} t_R: 23.2 min.

(*Z*)-1-Methyl-5-(2,3,4-trimethoxystyryl)-1*H*-indole-3-carboxylic acid (26): M.p.: 189-190ºC (MeOH). IR (KBr): 1660, 1520 cm^{-1}. ^1H NMR (400 MHz, $CDCl_3$): δ 3.92 (s, CH_3), 3.93 (s, CH_3), 3.94 (s, CH_3), 3.96 (s, CH_3), 6.72 (1H, d, *J* = 8.7), 7.20 (1H, d, *J* = 12.4), 7.33 (1H, d, *J* = 12.4), 7.31 (1H, d, *J* = 8.7), 7.35(1H, d, *J* = 8.7), 7.37 (1H, s), 7.57 (1H, d, *J* = 8.7), 7.84 (1H, s), 8.29 (1H, bs). ^{13}C NMR (100 MHz, $CDCl_3$): δ 33.6 (CH_3), 56.0 (CH_3), 60.8 (CH_3), 61.3 (CH_3), 106.3 (C), 107.8 (CH), 110.0 (CH), 120.4 (CH), 120.6 (CH), 121.1 (CH), 121.6 (CH), 124.9 (C), 127.1 (C), 128.9.1 (CH), 132.5 (C), 136.6 (CH), 136.8 (C), 142.4 (C), 151.5 (C), 152.9 (C), 169.9 (C) . HPLC: C_{18} t_R: 20.6 min.

(*Z*)-Methyl 1-methyl-5-(3,4,5-trimethoxystyryl)-1*H*-indole-3-carboxylate (27)

To a solution of the acid **25** (50 mg, 0.136 mmol) in MeOH (10 mL) (trimethylsilyl)diazomethane (2 mL) was added. After 15 min at room temperature, the solvent was evaporated obtaining compound **27** in quantitative yield. IR (film: 1699, 1570, 1503 cm^{-1}. ^1H NMR (400 MHz, $CDCl_3$): δ 3.62 (6H, s), 3.78 (3H, s), 3.84 (3H, s), 3.85 (3H, s), 6.49 (1H, d, *J* = 12.2), 6.54 (s, 2H), 6.65 (1H, d, *J* = 12.2), 7.20 (1H, d, *J* = 8.9), 7.25 (1H, d, *J* = 8.9), 7.73 (1H, s), 8.14 (1H, s). ^{13}C NMR (100 MHz, CDCl3): δ 33.5 (CH_3),

51.0 (CH_3), 55.9 (2) (CH_3), 60.9 (CH_3), 106.1 (2) (CH), 107.1 (C), 109.3 (CH), 122.2 (CH), 124.4 (CH), 126.4 (C), 128.8 (CH), 130.7 (CH), 131.0 (C), 133.1 (C), 135.6 (CH), 136.3 (C), 137.0 (C), 152.8 (2) (C), 165.4 (C). HRMS ($C_{22}H_{23}NO_5$ + Na): calcd. 404.1468 (M^+ + Na), found 404.1463. HPLC: C_{18} t_R: 21.6 min.

Preparation of compounds 28-31

A mixture of carboxilic acid **(25)** (1 mmol); 1 mmol of the corresponding aminoester: glycine ethyl ester hydrochloride, sarcosine methyl ester, β-alanine ethyl ester or dimethylamino malonate hydrochloride; 2 mmol of EDCI and 0.5 mmol of 4-DAMP were disolved in dry CH_2Cl_2 in inert atmosphere. After 72 h at room temperature, the reaction was treated with HCl 2N, extracted with CH_2Cl_2, washed with NaOH 2%, dried over anhydrous Na_2SO_4 and the solvent evaporated. The residue was purified by flash chromatography with hexane/EtOAc or crystallization yielding the compounds **28** (72%), **29** (55 %), **30** (54%) and **31** (30%) + **25** (20%).

(*Z*)-Ethyl 2-(1-methyl-5-(3,4,5-trimethoxystyryl)-1*H*-indole-3-carboxamido)acetate (28): IR (film): 3347, 1744, 1638, 1578 cm^{-1}. ^1H NMR (200 MHz, $CDCl_3$): δ 1.22 (3H, t, *J* = 7.2), 3.52 (3H, s), 3.76 (3H, s), 3.90 (2H, m), 4.14 (2H, c, *J* = 7.2), 6.41 (1H, d, *J* = 12.2), 6.46 (2H, s), 6.62 (1H, d, *J* = 12.2), 6.97 (1H, d, *J* = 8.6), 7.16 (1H, d, *J* = 8.6), 7.54 (1H, s), 8.01 (1H, s). ^{13}C NMR (50 MHz, $CDCl_3$): δ 14.2 (CH_3), 33.2 (CH_3), 41.3 (CH_3), 55.8 (CH_3), 60.9 (CH_3), 61.4 (CH_2), 106.0 (CH), 109.3 (C), 109,8 (CH), 121.5 (CH), 123.7 (CH), 125.8 (C), 128.7 (CH), 130.5 (C), 130.8 (CH), 132.5 (CH), 133.1 (C), 136.2 (C), 152.8 (C), 165.2 (C), 170.9 (C). HRMS ($C_{25}H_{28}N_2O_6$ + Na): calcd. 475.1839 (M^+ + Na), found 475.1861.

(*Z*)-Methyl 2-(N,1-dimethyl-5-(3,4,5-trimethoxystyryl)-1*H*-indole-3-carboxamido)acetate (29): IR (film): 3052, 2834, 1746, 1617, 1581 cm^{-1}. ^1H NMR (200 MHz, $CDCl_3$): δ 3.09 (3H, s), 3.58 (6H, s), 3.71 (3H, s), 3.78 (3H, s), 4.20 (2H, s), 6.44 (1H, d, *J* = 12.2), 6.47 (2H, s), 6.67 (1H, d, *J* = 12.2), 7.12 (1H, d, *J* = 8.8), 7.20 (1H, d, *J* = 8.8), 7.34 (1H, s), 7.72 (1H, s). ^{13}C NMR (50 MHz, $CDCl_3$): δ 33.1 (CH_3), 50.0 (CH_2), 52.0 (CH_3), 58.8 (CH_3), 60.7 (CH_3), 106.0 (CH), 109.2 (CH), 109.5 (C), 121.7 (CH),

123.7 (CH), 126.6 (C), 128.5 (CH), 130.1 (C), 130.8 (CH), 131.7 (CH), 133.1 (C), 135.6 (C), 136.8 (C), 157.7 (C), 167.5 (C), 170.0 (C). HRMS ($C_{25}H_{28}N_2O_6$ + Na): calcd. 475.1839 (M^+ + Na), found 475.1846.

(*Z*)-Ethyl 3-(1-methyl-5-(3,4,5-trimethoxystyryl)-1*H*-indole-3-carboxamido)propanoate (30): M.p.: 133-134ºC (MeOH). IR (KBr): 3359, 1727, 1611, 1579, 1512 cm^{-1}. ^1H NMR (200 MHz, $CDCl_3$): δ 1.28 (3H, t, *J* = 7.2), 2.64 (2H, t, *J* = 6.1), 3.61 (6H, s), 3.73 (2H, t, *J* = 6.1), 3.76 (3H, s), 3.82 (3H, s), 4.16 (2H, c, *J* = 7.2), 6.49 (1H, d, *J* = 12.2), 6.51 (2H, s), 6.73 (1H, d, *J* = 12.2), 7.15 (1H, d, *J* = 8.6), 1.25 (1H, d, *J* = 8.6), 7.59 (1H, s), 7.92 (1H, s). ^{13}C NMR (50 MHz, $CDCl_3$): δ 14.2 (CH_3), 33.2 (CH_3), 34.3 (CH_2), 34.8 (CH_2), 55.8 (CH_3), 60.6 (CH_2), 60.8 (CH3), 106, 0 (CH), 109.4 (CH), 121.4 (CH), 123.7 (CH), 125.7 (C), 128.7 (CH), 10.8 (CH), 132.2 (CH), 133.1 (C), 136.3 (C), 152.8 (C), 164.9 (C), 172.7 (C). HRMS ($C_{26}H_{30}N_2O_6$ + Na): calcd. 489.1996 (M^+ + Na), found 489.2021.

(*Z*)-Dimethyl 2-(1-methyl-5-(3,4,5-trimethoxystyryl)-1*H*-indole-3-carboxamido)malonate (31). IR (KBr): 1742, 1629, 1576 cm^{-1}. ^1H NMR (200 MHz, $CDCl_3$): δ 3.61 (6H, s), 3.76 (3H, s), 3.81 (3H, s), 3.86 (6H, s), 6.42 (1H, d, *J* = 6.6), 6.48 (1H, d, *J* = 12.0), 6.50 (2H, s), 6.68 (1H, d, *J* = 12.0), 6.88 (1H, d, *J* = 6.6), 7.13 (1H, d, *J* = 8.6), 7.24 (1H, d, *J* = 8.6), 7.66 (1H, s), 8.19 (1H, s).

Preparation of compounds 32-34

The compounds **28-30** were saponificated by treatment with KOH/MeOH 10% during 30' at rt. Yielding thecompounds **32** (77%), **33** (84%) and **34** (90%) were obtained.

(*Z*)-2-(1-methyl-5-(3,4,5-trimethoxystyryl)-1*H*-indole-3-carboxamido)acetic acid (32): M.p.: 144-145ºC (MeOH). IR (KBr): 3412, 1735, 1640, 1578 cm^{-1}. ^1H NMR (200 MHz, CD_3OD): δ 3.45 (3H, s), 3.62 (3H, s), 3.72 (3H, s), 3.97 (2H, s), 6.40 (1H, d, *J* = 12.2), 6.46 (2H, d), 7.09 (1H, d, *J* = 8.6), 7.24 (1H, d, *J* = 8.6), 7.71 (1H, s), 7.99 (1H, s). ^{13}C NMR (50 MHz, CD_3OD): δ 33.4 (CH_3), 41.7 (CH_2), 56.2 (CH_3), 61.0 (CH_3), 107.4 (CH), 110.6 (CH), 110.0 (C), 122.6 (CH), 124.9 (CH), 127.6 (C), 129.9 (CH), 131.9 (CH), 133.8 (CH), 134.6 (C), 137.8 (C), 154.0 (C), 167.8 (C), 173.6 (C). HRMS

($C_{23}H_{24}N_2O_6$ + Na): calcd. 447.1526 (M^+ + Na), found 447.15.39.

(*Z*)-2-(*N*,1-dimethyl-5-(3,4,5-trimethoxystyryl)-1*H*-indole-3-carboxamido)acetic acid (33): IR (KBr): 3399, 3431, 1584, 1500 cm^{-1}. ^1H NMR (200 MHz, CD_3OD): δ 3.02 (3H, s), 3.40 (3H, s), 3.61 (3H, s), 3.68 (3H, s), 3.95 (3H, s), 6.37 (1H, d, *J* = 12.2), 6.43 (2H, s), 6.60 (1H, d, *J* = 12.2), 7.08 (1H, d, *J* = 8.6), 7.20 (1H, d, *J* = 8.6), 7.40 (1H, bs), 7.70 (1H, s). ^{13}C NMR (50 MHz, CD_3OD): δ 33.2 (CH_3), 37.5 (CH_3), 51.0 (CH_2), 56.2 (CH_3), 61.0 (CH_3), 107.4 (CH), 110.3 (CH), 110.5 (C), 122.5 (CH), 124.8 (CH), 128.2 (C), 129.8 (CH), 131.5 (C), 131.9 (CH), 134.7 (C), 137.1 (C), 138.0 (C), 154.0 (C), 169.8 (C), 177.7 (C). HRMS ($C_{24}H_{26}N_2O_6$ + Na): calcd. 461.1683 (M^+ + Na), found 461.1658.

(*Z*)-3-(1-methyl-5-(3,4,5-trimethoxystyryl)-1*H*-indole-3-carboxamido)propanoic acid (34): M.p.: 169-170ºC (CH_2Cl_2/MeOH). IR (KBr): 3378, 1726, 1606, 1577, 1506 cm^{-1}. ^1H NMR (200 MHz, $CDCl_3$): δ 2.60 (2H, s), 3.60 (6H, s), 3.70 (2H, m), 3.74 (3H, s), 3.80 (3H, s), 6.48 (1H, d, *J* = 12.2), 6.52 (2H, s), 6.70 (1H, d, *J* = 12.2), 7.16 (1H, d, *J* = 8.2), 7.24 (1H, d, *J* = 8.2), 7.65 (1H, s), 7.85 (1H, s). ^{13}C NMR (50 MHz, $CDCl_3$): δ 33.8 (CH_3), 34.3 (CH_2), 34.9 (CH_2), 55.9 (CH_3), 60.9 (CH_3), 106.0 (CH), 109.6 (CH), 110.2 (C), 120.2 (CH), 124.0 (CH), 125.1 (C), 128.9 (CH), 130.6 (CH), 130.7 (C), 133.1 (CH), 133.3 (C), 136.4 (C), 152.9 (C), 165.4 (C), 176.0 (C). HRMS ($C_{24}H_{26}N_2O_6$ + Na): calcd. 461.1683 (M^+ + Na), found 461.1696.

3-Bromo-1-methyl-5-(3,4,5-trimethoxystyryl)-1*H*-indole (35)

To a suspension of triphenyl(3,4,5-trimethoxybenzyl)phosphonium bromide (3.02 g, 5.80 mmol) in dry THF (40 mL), at -40ºC in argon atmosphere, *n*BuLi (1.6 M in hexane, 3.4 mL, 5.5 mmol) was added and stirred for 1 h. A solution of compound **5** (1.06 g, 4.45 mmol) in dry THF (15 mL) was slowly added at -40 ºC and progressively warmed to room temperature. After 24 h, the reaction mixture was poured into ammonium chloride solution and extracted with CH_2Cl_2. The organic layers were washed to neutrality with brine, dried over anhydrous Na_2SO_4, filtered and evaporated to dryness. After chromatography on silica gel (Hex/AcOEt 7/3), 260 mg (0.65 mmol, 15%) of **35*Z*** and 989 mg (2.46 mmol, 55%) of **35*E*** were obtained.

(*Z*)-3-Bromo-1-methyl-5-(3,4,5-trimethoxystyryl)-1*H*-indole (35*Z*): IR (film): ^{1}H NMR (200 MHz, $CDCl_3$): δ 3.65 (6H, s), 3.75 (3H, s), 3.84 (3H, s), 6.47 (1H, d, *J* = 12.2), 6.56 (2H, s), 6.70 (1H, d, *J* = 12.2), 7.04 (1H, s), 7.14 (1H, d, *J* = 8.6), 7.23 (1H, dd, *J* = 8.6 and 1.2), 7.55 (1H, d, *J* = 1.2). ^{13}C NMR (50 MHz, CDCl3): δ 33.3 (CH_3), 56.1 (2) (CH_3), 61.0 (CH_3), 89.8 (C), 106.1 (2) (CH), 109.1 (CH), 119.9 (CH), 124.2 (CH), 128.1 (CH), 128.6 (CH), 129.1 (C), 129.8 (2) (C), 130.6 (CH), 132.9 (C), 135.4 (C), 137.3 (C), 153.5 (2) (C). HRMS HPLC: C_{18} t_R: 26.3 min.

(*E*)-3-Bromo-1-methyl-5-(3,4,5-trimethoxystyryl)-1*H*-indole (35*E*)

IR (film): 1578, 1503, 1170 cm^{-1}. ^{1}H NMR (200 MHz, $CDCl_3$): δ 3.70 (3H, s), 3.88 (3H, s), 3.93 (6H, s), 6.77 (2H, s), 7.04 (1H, d, *J* = 16.4), 7.14 (1H, s), 7.18 (1H, d, *J* = 16.4), 7.26 (1H, d, *J* = 8.8), 7.48 (1H, dd, *J* = 8.8 and 1.6), 7.66 (1H, d, *J* = 1.6). ^{13}C NMR (50 MHz, CDCl3): δ 33.2 (CH_3), 56.2 (2) (CH_3), 61.0 (CH_3), 89.7 (C), 103.3 (2) (CH), 109.9 (CH), 117.7 (CH), 121.3 (CH), 126.7 (CH), 127.7 (CH), 128.4 (CH), 129.1 (2) (C), 129.7 (C), 133.7 (C), 136.1 (C), 153.4 (2) (C).

2,3-Dibromo-1-methyl-5-(3,4,5-trimethoxystyryl)-1*H*-indole (36)

To a suspension of triphenyl(3,4,5-trimethoxybenzyl)phosphonium bromide (1.07 g, 2.05 mmol) in dry THF (40 mL), at -40ºC in argon atmosphere, *n*BuLi (1.6 M in hexane, 1.2 mL, 1.92 mmol) was added and stirred for 1 h. A solution of compound **5** (500 mg, 1.58 mmol) in dry THF (10 mL) was slowly added at -40 ºC and progressively warmed to room temperature. After 24 h, the reaction mixture was poured into ammonium chloride solution and extracted with CH_2Cl_2. The organic layers were washed to neutrality with brine, dried over anhydrous Na_2SO_4, filtered and evaporated to dryness. After chromatography on silica gel (Hex/AcOEt 8/2 and 6/4), 324 mg (0.67 mmol, 42.4%) of **36*Z*** and 174 mg (0.36 mmol, 23%) of a mixture **36*Z*/36*E*** were obtained.

(*Z*)-2,3-Dibromo-1-methyl-5-(3,4,5-trimethoxystyryl)-1*H*-indole (36*Z*): IR (film): 1580, 1503, 1170 cm^{-1}. ^{1}H NMR (200 MHz, $CDCl_3$): δ 3.64 (6H, s), 3.77 (3H, s); 3.84 (3H, s), 6.44 (1H, d, *J* = 12.0), 6.52 (2H, s), 6.68 (1H, d, *J* = 12.0), 7.16 (1H, d, *J* = 8,8); 7,21 (1H, dd, *J* = 8.8 and 1.4), 7.49 (1H, d, *J* = 1.4).

^{13}C NMR (50 MHz, CDCl3): δ 32.3 (CH_3), 55.9 (2) (CH_3), 60.9 (CH_3), 92.7 (C), 106.1 (2) (CH), 109.2 (CH), 115.0 (C), 119.1 (CH), 124.4 (CH), 126.7 (CH), 128.9 (CH), 129.8 (C), 130.2 (C), 132.9 (C), 135.4 (C), 137.3 (C), 152.9 (2) (C). HRMS HPLC: C_{18} t_R: 25.4 min.

(*E*)-2,3-Dibromo-1-methyl-5-(3,4,5-trimethoxystyryl)-1*H*-indole (36*E*): ^{1}H NMR (200 MHz, $CDCl_3$): δ 3.68 (3H, s), 3.89 (3H, s), 3.91 (6H, s), 6.74 (2H, s), 7.00 (1H, d, *J* = 16.4), 7,10 (1H, d, *J* = 16.4), 7.15 (1H, d, *J* = 8.8), 7.39 (1H, bs, *J* = 8.8), 7.56 (1H, bs). ^{13}C NMR (50 MHz, CDCl3): δ 32.3 (CH_3), 56.1 (2) (CH_3), 60.9 (CH_3), 92.8 (C), 103.3 (2) (CH), 109.9 (CH), 115.2 (C), 116.9 (CH), 121.4 (CH), 126.9 (CH), 127.1 (C), 128.5 (CH), 130.3 (C), 133.4 (C), 135.9 (C), 137.7 (C), 153.4 (2) (C) HRMS HPLC: C_{18} t_R: 21.5 min.

(*Z and E*)-1-Methyl-5-(3,4,5-trimethoxystyryl)-1*H*-benzo[*d*]imidazole (37*Z* and 37*E*) and (*Z and E*)-1-methyl-6-(3,4,5-trimethoxystyryl)-1*H*-benzo[*d*]imidazole (38*Z* and 38*E*).

(3,4,5-trimethoxybenzyl)triphenylphosphonium bromide (1.38 g, 2.63 mmol) was suspended in THF (18 mL) and cooled to -40 ºC under Ar, then *n*BuLi (1.6 M in hexane, 1.8 mL, 2.88 mmol) was added dropwise and the resulting solution was stirred for 1 h. A solution of a 1:1 mixture of 1*H*-benzimidazol-5-carbaldehyde and 1*H*-benzimidazol-6-carbaldehyde (383 mg, 2.39 mmol) in THF (15 mL) was added and warm to room temperature. Once completed, the reaction mixture was cooled to 0 ºC, quenched with some drops of water and extracted with dichloromethane. The organic layers were washed with brine, dried over anhydrous Na_2SO_4, and evaporated to give the crude of the reaction (1.48 g), which after chromatography on silica gel afforded one fraction of 1:1 mixture containing the *Z*-isomers of 1-methyl-5-(3,4,5-trimethoxystyryl)-1*H*-benzo[*d*]imidazole and 1-methyl-6-(3,4,5-trimethoxystyryl)-1*H*-benzo[*d*] imidazole (206 mg, 24%) and another 1:1 mixture containing the *E*-isomers of 1-methyl-5-(3,4,5-trimethoxystyryl)-1*H*-benzo[*d*]imidazole and 1-methyl-6-(3,4,5-trimethoxystyryl)-1*H*-benzo[*d*] imidazole (326 mg, 38%).

(Z)*-1-methyl-5-(3,4,5-trimethoxystyryl)-1*H*-benzo[*d*]imidazole (37*Z*) *and* *(Z)*-1-Methyl-6-(3,4,5-trimethoxystyryl)-1*H*-benzo[*d*]imidazole** (**38*Z). IR (film): cm^{-1}. *Major isomer:* ^{1}H NMR (400 MHz, $CDCl_3$): δ 3.60 (6H, s), 3.74 (3H, s), 3.82 (3H, s), 6.49 (2H, s), 6.52 (1H, d, *J* = 12,1), 6.72 (1H, d, *J* = 12,1), 7.22 (1H, d, *J* = 8,6), 7.29 (1H, s), 7.66 (1H, d, *J* = 8,6), 7.83 (1H, s). ^{13}C NMR (100 MHz, $CDCl_3$): δ 30.9 (CH_3), 55.8 (2) (CH_3), 60.9 (CH_3), 106.0 (2) (CH), 109.6 (CH), 119.8 (CH) , 123.7 (CH), 129.6 (CH), 130.2 (CH), 131.6 (C), 132.3 (C), 132.6 (C), 132.8 (C), 137.2 (C), 144.1 (CH), 152.8 (2) (C). *Minor isomer:* ^{1}H NMR (400 MHz, $CDCl_3$): δ 3.61 (6H, s), 3.81 (3H, s), 3.83 (3H, s), 6.50 (1H, d, *J* = 12.1), 6.50 (2H, s), 6.71 (1H, d, *J* = 12.1), 7.27 (1H, s), 7.29 (1H, d, *J* = 8.6), 7.65 (1H, m), 7.75 (1H, s). ^{13}C NMR (100 MHz, $CDCl_3$): δ 31.1 (CH_3), 56.1 (2) (CH_3), 60.9 (CH_3), 106.0 (2) (CH), 108.8 (CH), 120.7 (CH), 124.4 (CH), 129.1 (CH), 130.3 (CH), 144.0 (CH), 153.4 (2) (C), five (C) were not observed. HRMS ($C_{19}H_{20}N_2O_3$+Na): calcd. 347.1366 (M^++Na^+), found 347.1365. HPLC: C_{18} t_R: 13.83 and 13.93 min. (7:3). C_8 t_R: 13.08 and 13.14 min. (7:3). Phenylic t_R: 13.52 and 13.68 min. (7:3)

(E)*-1-methyl-5-(3,4,5-trimethoxystyryl)-1*H*-benzo[*d*]imidazole (37*E*) *or* *(E)*-1-methyl-6-(3,4,5-trimethoxystyryl)-1*H*-benzo[*d*]imidazole** (**38*E). IR (film): cm^{-1}. ^{1}H NMR (400 MHz, $CDCl_3$): δ 3.84 (3H, s), 3.87 (3H, s), 3.92 (6H, s), 6.76 (2H, s), 7.05 (1H, d, *J* = 16.4), 7.16 (1H, d, *J* = 16.4), 7.47 (1H, bs) , 7.49 (1H, dd, *J* = 8.4 and 1.8), 7.75 (1H, d, *J* = 8.4), 7.85 (1H, s). ^{13}C NMR (100 MHz, $CDCl_3$): δ 31.2 (CH_3), 56.2 (2) (CH_3), 61.0 (CH_3), 106.1 (2) (CH), 107.4 (CH), 120.2 (CH), 121.2 (CH), 128.0 (CH), 128.6 (CH), 132.8 (C), 133.3 (C), 135.1 (C), 137.9 (C), 144.1 (CH), 143.4 (C), 153.5 (2) (C). HRMS ($C_{19}H_{20}N_2O_3$+Na): calcd. 347.1366 (M^++Na^+), found 347.1362. HPLC: C_{18} t_R: 13.79 min. C_8 t_R: 12.86 min. Phenylic t_R: 13.42 min.

Determination of Aqueous Solubility

The aqueous solubility of the compounds was determined using an approach based on the saturation

shake-flask method. Approximately 2 mg of each compound was suspended in 0.3 mL pH 7.0 buffer in a glass vial and shaken 72 h at room temperature. The resulting mixture was filtrated over a 22 µm filter to discard the insoluble residues and the concentration in the supernatant was measured by UV absorbance in a Helios Alfa Spectrophotometer. Previously, for each compound the maximum wavelength of absorbance is determined and a calibration line is performed.

Inhibition of tubulin polymerization

Bovine brain tubulin was isolated as previously described.[13] The assays were carried out at pH 6.7 with 1.5 mg/mL protein and the measured ligand concentration in 0.1 M MES buffer, 1 mM EGTA, 1 mM $MgCl_2$, 1 mM β-ME, 1.5 mM GTP. The samples were incubated at 20 °C for 30 min and subsequently cooled on ice for 10 min. Tubulin polymerization was monitored by measuring the absorbance increase in the UV at 450 nm caused by a temperature shift from 4 ºC to 37 ºC. After reaching a stable plateau, temperature was switched back to 0 ºC and return to the initial absorption values was ascertained, in order to confirm the reversible nature of the monitored process. The difference in amplitude between the stable plateau and the initial baseline of the curves was taken as the degree of tubulin assembly for each experiment. Comparison with control curves with identical conditions but without ligands yielded tubulin polymerization inhibition as a percentage value. Initially, all compounds were assayed at a concentration of 5 µM in at least two independent measurements, and those displaying a TPI higher than 40% were selected for further studies. The tubulin polymerization inhibitory activity of the selected compounds was measured at different ligand concentrations and, as expected, the extent of inhibition by all compounds increased monotonically with the mole ratio of the total ligand to total tubulin in the solution. The obtained values were fitted to monoexponential curves and the IC_{50} values of tubulin polymerization inhibition were calculated from the best fitting curves.

Cell culture. HL-60 (human acute myeloid leukemia) cell line was grown in RPMI-1640 culture

medium containing 10% (v/v) heat-inactivated fetal bovine serum (FBS), 2 mM L-glutamine, 100 U/mL penicillin, and 100 μg/mL streptomycin at 37 °C in humidified 95% air and 5% CO2. A549 (human non-small lung carcinoma), HeLa (human cervical carcinoma), and HT-29 (human colon carcinoma) cell lines were grown in DMEM culture medium containing 10% (v/v) heat-inactivated fetal bovine serum (FBS), 2 mM L-glutamine, 100 U/mL penicillin, and 100 μg/mL streptomycin at 37 °C in humidified 95% air and 5% CO2. Cells were periodically tested for *Mycoplasma* infection and found to be negative.

Cell Growth Inhibition Assay. The effect of the different compounds on the proliferation of human tumor cell lines (cytostatic activity) was determined as previously described[21] using the XTT (sodium 3′-[1-(phenylaminocarbonyl)-3,4-tetrazolium]-bis(4-methoxy-6-nitro)-benzenesulfonic acid hydrate) cell proliferation kit (Roche Molecular Biochemicals, Mannheim, Germany) according to the manufacturer's instructions. Cells (1.5×10^3 A549, HeLa, HT-29, and 3×10^3 HL-60 in 100 μL) were incubated in culture medium containing 10% heat-inactivated FBS in the absence and in the presence of the indicated compounds at different concentration ranges from 10^{-5} to 10^{-13} M, in 96-well flat-bottomed microtiter plates, and following 72 h of incubation at 37 °C in a humidified atmosphere of air/CO2 (19/1), the XTT assay was performed. Measurements were performed in triplicate, and each experiment was repeated three times. The IC_{50} (50% inhibitory concentration) value, defined as the drug concentration required to cause 50% inhibition in cellular proliferation with respect to the untreated controls, was determined for each compound. Nonlinear curves fitting the experimental data were carried out for each compound.

Cell Cycle Analysis. For cell cycle analyses, untreated and drug-treated HeLa cells ($(2-4) \times 10^5$) were centrifuged and fixed overnight in 70% ethanol at 4 °C. Then cells were washed three times with PBS, incubated for 1 h with 1 mg/mL RNase A and 20 μg/mL propidium iodide at room temperature, and

analyzed with a Becton Dickinson fluorescence-activated cell sorter (FACSCalibur) flow cytometer (San Jose, CA) as described previously.[27, 28] Quantification of apoptotic cells was calculated as the percentage of cells in the sub-G_0/G_1 peak in cell cycle analysis.[27, 28]

Confocal Microscopy. HeLa cells were grown on 0.01% poly-L-lysine coated coverslips, and after drug treatment, the coverslips were washed three times with HPEM buffer (25 mM HEPES, 60 mM PIPES, 10 mM EGTA, 3 mM $MgCl_2$, pH 6.6), fixed with 4% paraformaldehyde in HPEM buffer for 15 min, and permeabilized with 0.5% Triton X-100 as previously described.[14] Coverslips were incubated with a specific Ab-1 anti-α-tubulin mouse monoclonal antibody (diluted 1:150 in PBS) (Calbiochem, San Diego, CA) for 1 h, washed four times with PBS, and then incubated with CY3-conjugated sheep antimouse IgG (diluted 1:100 in PBS) (Jackson ImmunoResearch, West Grove, PA) for 1 h at 4 °C. After being washed four times with PBS, cell nuclei were stained with DAPI (Sigma, St. Louis, MO) for 5−10 min and washed with PBS, and then the samples were analyzed by confocal microscopy using a ZeissLSM 310 laser scan confocal microscope. A drop of SlowFade light antifading reagent (Molecular Probes, Eugene, OR) was added to preserve fluorescence. Negative controls, lacking the primary antibody or using an irrelevant antibody, showed no staining.

Western Blot. About 5×10^6 cells were pelleted by centrifugation, washed with PBS, lysed, and subjected to Western blot analysis as described previously.[27] Proteins were separated through SDS polyacrylamide gels under reducing conditions, transferred to nitrocellulose filters, blocked with 5% defatted milk powder, and incubated overnight with anti-activated caspase-3 (1:1000 dilution) rabbit monoclonal antibody, which detects the full-length (35 kDa) and large fragment (17/19 kDa) of caspase-3 (Cell Signaling Technology, Danvers, MA), or anti-poly(ADP-ribose) polymerase (PARP) (1:1000 dilution) rabbit monoclonal antibody that detects the full-length PARP-1 and the large fragment (89 kDa) produced by casopase cleavage (Cell Signaling Technology). Signals were developed using an

enhanced chemiluminescence detection kit (Amersham Biosciences, Aylesbury, UK). Immunoblotting with AC-15 anti-42 kDa β-actin (1:5000 dilution) mouse monoclonal antibody (Sigma) was used as an internal loading control, revealing equivalent amounts of protein in each lane of the gel. Prestained protein molecular mass standards (Bio-Rad) were run in parallel.

Chemical Structure. Calculations were performed at the molecular mechanics level (MMFF94s), semiempirical level (AM1), and HF and B3LYP 6-31+G* DFT levels using the Spartan 08 and Gaussian G03 software packages. Conformational analyses with the MMFF94s forcefield were performed by systematically rotating in 18° steps the bonds between the bridges and the pending aromatic rings. The phenyl rings of the trimethoxybenzene rings obtained were superimposed over one another and over the trimethoxyphenyl ring of combretastatin A4 extracted from the X-ray crystal structure with tubulin (pdb: 5LYJ), and the conformations for which the phenyl ring of the indoles covered a region closer to the 3-hydroxy-4-methoxyphenyl ring of combretastatin A4 were subjected to further unrestrained energy minimization steps at the semiempirical (AM1), 6-31G** HF, and then B3LYP/6-31+G* DFT levels of theory. The conformations were then superimposed again onto combretastatin A4 by means of the Spartan 08 pharmacophore option, by selecting as pharmacophoric references the two aromatic rings of combretastatin A4 (hydrophobic), the two external oxygens of the trimethoxyphenyl moiety (hydrogen-bond acceptors), and the excluded volume, as calculated from the complex of combretastatin A4 with tubulin.

Docking Experiments. The pdb structure data of the tubulin − combretastatin A4 complex (5LYJ.pdb)[26] and 15 more complexes of colchicine site ligands with tubulin (1SA1.pdb, 3HKC,pdb, 3HKD.pdb, 3HKE.pdb, 3N2G.pdb, 3N2K.pdb, 3UT5.pdb, 4O2A.pdb, 4O2B.pdb, 4YJ2.pdb, 4YJ3.pdb, 5C8y.pdb, 5CA0.pdb, 5CA1.pdb, 5GON.pdb, 5CB4.pdb) were retrieved[29] and chains C−E were removed. Five additional tubulin models were built from 1SA1.pdb after energy minimization and

molecular dynamics simulations at 300 K, initially with a restrained backbone and then with an unrestrained one using AMBER14[30] and representative structures were selected as previously described.[31] The ligands were built with Spartan 08, prepared with AutodockTools and docked with AutoDock 4.2,[32, 33] by running the Lamarckian genetic algorithm (LGA) 100−300 times with a maximum of 2.5×10^6 energy evaluations, 150 individuals in the population, and a maximum of 27000 generations, PLANTS[34] and DOCK3.7[35]. The results were analyzed with AutoDockTools,[32, 33] with Marvin,[36] OpenEye[37] and with JADOPPT.[38] Docking poses were selected if they were found by at least two docking programs using different scoring functions and based on the scoring.

FIGURE LEGENDS

Figure 1. Representative combretastatin type ligands

Figure 2. Effects of compounds **17**, **21** and **23** on the microtubule network of Hela cells. Cells were incubated in the absence (Control) or in the presence of 10 or 100 nM of compounds **17**, **21** and **23** for 15 h and then fixed and processed to analyze microtubules (red fluorescence) and nuclei (blue fluorescence) as described in the Experimental Section. Bar: 25 μm. The photomicrographs shown are representative of at least three independent experiments performed.

Figure 3. Effect of different compounds on the distinct cell cycle phases in HeLa cells. Compounds **16E**, **17**, **21**, **23**, **25**, **27** and **30** were incubated for 15 h and then their DNA content was analyzed by flow cytometry as described in the Experimental Section. The different cell cycle phases were quantified and represented in pie charts to easily visualize the changes in G_2/M arrest. Untreated control cells were run in parallel. Data shown are representative of at least three independent experiments performed.

Figure 4. Time-course of the effects of compounds **21** and **23** on cell cycle in HeLa cells. Cells were incubated with 1 or 10 nM of **21** and **23** for the indicated times, and their DNA content was analyzed by fluorescence flow cytometry. The positions of the G_0/G1 and G_2/M peaks are indicated by arrows, and the proportion of cells in each phase of the cell cycle was quantified by flow cytometry. The cell population in the sub-G_0/G1 region represents cells with hypodiploidal DNA, an indicator of apoptosis, and the percentages of cells at this region are indicated in each histogram. Untreated control cells were run in parallel. The experiments shown were representative of three performed.

Figure 5. Effect of verapamil on the sensitivities of A549 cancer cells to **21** and **23**. Cells were co-incubated with verapamil and different concentrations of **21** and **23**. The dose–response curves were drawn using the GraphPad Prism 5 software. Results are mean values ± S.D. of a representative experiment carried out in triplicate, out of three performed.

Figure **6** Best superpositions of the X-ray structure of combretastatin A4 (in cyan) in the complex with tubulin and the conformations of representative compounds showing the effects of the structural modifications and the corresponding docking results (the protein is shown in grey): a) with **15**; b) with **23**; c) with **24**; d) with the 11,diarylethene isomer (isocombretastatin) of **15** and e) with the 11,diarylethene isomer (isocombretastatin) of **24** and f) a combination of b,c and e.

Scheme 1: Synthesis of 3-indolecarbaldehyde combretastatin derivatives 13-16 and bromoderivatives 35 and 36.[a]

(a) (i) $(3,4,5\text{-}(MeO)_3PhCH_2)Ph_3PBr$ (**11**), THF, BuLi (1.6M), THF, -40ºC, 1h; (ii) 1-ethyl-1*H*-indole-5-carbaldehyde (**1**), 1-methyl-1*H*-indole-5-carbaldehyde (**2**), 1-ethyl-1*H*-indole-3,5-dicarbaldehyde (**3**), 1-methyl-3-bromo-1*H*-indole-5-carbaldehyde (**4**) or 1-methyl-2,3-dibromo -1*H*-indole -5-carbaldehyde

(**5**), THF, -40 ºC to rt, 24 h. (b) (i) (2,3,4-$(MeO)_3PhCH_2$)Ph_3PBr (**12**), THF, BuLi (1.6M), THF, -40ºC, 1h; (ii) 1-methyl-1*H*-indole-5-carbaldehyde (**2**), THF, -40 ºC to rt, 24 h.

Scheme 2: Preparation of benzimidazole combretastatin derivatives 37+38.[a]

Reagents and conditions: (a) (i) Ph_3P(3,4,5-MeO_3PhCH_2)I, THF, *n*BuLi (1.6M), THF, -40 ºC, 1h; (ii) 1-methyl-1*H*-benzimidazole-5(6)-carbaldehydes, THF, -40 ºC to rt, 24 h.

Scheme 3: Preparation of 3-substituted indole-combretastatin derivatives 17-34.[a]

Reagents and conditions: (a) (i) $POCl_3$, DMF, 0 ºC, 1 h; (ii) **15** or **16**, 60 ºC, 2 h. (b) $NaBH_4$, MeOH, rt, 30 min. (c) $NH_2OH{\cdot}HCl$, MeOH, pyr (2 drops), rt, 24 h. (d) Ac_2O, pyr, rt, 4 h. (e) **17** or **18** in *t*BuOH, 2-methyl-2-butene, THF; add $NaClO_2$, NaH_2PO_4, H_2O, rt, 12 h. (f) $TMSCHN_2$, MeOH, 15 min. (g) (i) $NH_2CH_2COOEt{\cdot}HCl$; EDCI; 4-DMAP; rt, 48 h, inert atmosphere. (h) $CH_3NHCH_2COOMe{\cdot}HCl$; EDCI; 4-DMAP; rt, 48 h, inert atmosphere. (i) $NH_2CH_2CH_2COOEt$; EDCI; 4-DMAP; rt, 48 h, inert atmosphere. (j) $(COOMe)_2CHNH_2{\cdot}HCl$; EDCI; 4-DMAP; rt, 48 h, inert atmosphere. (k) KOH/MeOH, rt, 30 min.

Table 1. Aqueous solubility of representative compounds in aqueous buffer pH 7.0

Table 2. Tubulin Polymerization Inhibitory Activity, Cytotoxic Activity against Human Cancer Cell Lines, and Results of the Docking Studies.

ACKNOWLEDGEMENTS

This work was supported by the Consejería de Educación de la Junta de Castilla y León (SA030U16) cofunded by the EU's European Regional Development Fund - FEDER. Different parts of the work were performed on the basis of financial support from the Spanish Ministerio de Economía y Competitividad (SAF2014-59716-R and SAF2017-89672-R), and the Instituto de Salud Carlos III

(RD12/0036/0065 from Red Temática de Investigación Cooperativa en Cáncer, cofunded by the EU's European Regional Development Fund - FEDER). We thank the people at Asocarsa S.A. slaughter-house for providing us with the calf brains.

REFERENCES

1. Dumontet, C.; Jordan, M. A. Microtubule-binding agents: a dynamic field of cancer therapeutics. *Nat Rev Drug Discov* **2010,** 9, 790-803.
2. Mollinedo, F.; Gajate, C. Microtubules, microtubule-interfering agents and apoptosis. *Apoptosis* **2003,** 8, 413-50.
3. Komlodi-Pasztor, E.; Sackett, D.; Wilkerson, J.; Fojo, T. Mitosis is not a key target of microtubule agents in patient tumors. *Nat Rev Clin Oncol* **2011,** 8, 244-50.
4. Lippert, J. W., 3rd. Vascular disrupting agents. *Bioorg Med Chem* **2007,** 15, 605-15.
5. Perez-Perez, M. J.; Priego, E. M.; Bueno, O.; Martins, M. S.; Canela, M. D.; Liekens, S. Blocking Blood Flow to Solid Tumors by Destabilizing Tubulin: An Approach to Targeting Tumor Growth. *J Med Chem* **2016,** 59, 8685-8711.
6. Lunt, S. J.; Akerman, S.; Hill, S. A.; Fisher, M.; Wright, V. J.; Reyes-Aldasoro, C. C.; Tozer, G. M.; Kanthou, C. Vascular effects dominate solid tumor response to treatment with combretastatin A-4-phosphate. *Int J Cancer* **2011,** 129, 1979-89.
7. Siemann, D. W. The unique characteristics of tumor vasculature and preclinical evidence for its selective disruption by Tumor-Vascular Disrupting Agents. *Cancer Treat Rev* **2011,** 37, 63-74.
8. Liang, W.; Ni, Y.; Chen, F. Tumor resistance to vascular disrupting agents: mechanisms, imaging, and solutions. *Oncotarget* **2016,** 7, 15444-59.
9. Tozer, G. M.; Kanthou, C.; Lewis, G.; Prise, V. E.; Vojnovic, B.; Hill, S. A. Tumour vascular disrupting agents: combating treatment resistance. *Br J Radiol* **2008,** 81 Spec No 1, S12-20.
10. Malebari, A. M.; Greene, L. M.; Nathwani, S. M.; Fayne, D.; O'Boyle, N. M.; Wang, S.; Twamley, B.; Zisterer, D. M.; Meegan, M. J. beta-Lactam analogues of combretastatin A-4 prevent metabolic inactivation by glucuronidation in chemoresistant HT-29 colon cancer cells. *Eur J Med Chem* **2017,** 130, 261-285.
11. Greene, L. M.; O'Boyle, N. M.; Nolan, D. P.; Meegan, M. J.; Zisterer, D. M. The vascular targeting agent Combretastatin-A4 directly induces autophagy in adenocarcinoma-derived colon cancer cells. *Biochem Pharmacol* **2012,** 84, 612-24.
12. Quan, H.; Liu, H.; Li, C.; Lou, L. 1,4-Diamino-2,3-dicyano-1,4-bis(methylthio)butadiene (U0126) enhances the cytotoxicity of combretastatin A4 independently of mitogen-activated protein kinase kinase. *J Pharmacol Exp Ther* **2009,** 330, 326-33.
13. Alvarez, R.; Puebla, P.; Diaz, J. F.; Bento, A. C.; Garcia-Navas, R.; de la Iglesia-Vicente, J.; Mollinedo, F.; Andreu, J. M.; Medarde, M.; Pelaez, R. Endowing indole-based tubulin inhibitors with an anchor for derivatization: highly potent 3-substituted indolephenstatins and indoleisocombretastatins. *J Med Chem* **2013,** 56, 2813-27.
14. Maya, A. B.; Perez-Melero, C.; Mateo, C.; Alonso, D.; Fernandez, J. L.; Gajate, C.; Mollinedo, F.; Pelaez, R.; Caballero, E.; Medarde, M. Further naphthylcombretastatins. An investigation on the role of the naphthalene moiety. *J Med Chem* **2005,** 48, 556-68.
15. Campaigne, E.; Archer, W. L. Formylation of dimethylaniline. *Org Syn Coll* **1963,** 4, 331-2.
16. Alvarez, C.; Alvarez, R.; Corchete, P.; Perez-Melero, C.; Pelaez, R.; Medarde, M. Naphthylphenstatins as tubulin ligands: synthesis and biological evaluation. *Bioorg Med Chem* **2008,** 16, 8999-9008.
17. Alvarez, C.; Alvarez, R.; Corchete, P.; Lopez, J. L.; Perez-Melero, C.; Pelaez, R.; Medarde, M.

Diarylmethyloxime and hydrazone derivatives with 5-indolyl moieties as potent inhibitors of tubulin polymerization. *Bioorg Med Chem* **2008,** 16, 5952-61.
18. Zuzana Čurillová, Z.; Kutschy, P.; Solčániová, E.; Pilátová, M.; Ján Mojžiš, J.; Kováčikd, V. Synthesis and antiproliferative activity of 1-methoxy-1-(α-D-ribofuranosyl)- and 1-(β-D-ribofuranosyl)brassenin B. *ARKIVOC* **2008,** viii, 85-104.
19. Jones, J. *The chemical synthesis of peptides*. Claredon Press: Oxford, 1994.
20. Chen, J.; Wang, Z.; Li, C. M.; Lu, Y.; Vaddady, P. K.; Meibohm, B.; Dalton, J. T.; Miller, D. D.; Li, W. Discovery of novel 2-aryl-4-benzoyl-imidazoles targeting the colchicines binding site in tubulin as potential anticancer agents. *J Med Chem* **2010,** 53, 7414-27.
21. David-Cordonnier, M. H.; Gajate, C.; Olmea, O.; Laine, W.; de la Iglesia-Vicente, J.; Perez, C.; Cuevas, C.; Otero, G.; Manzanares, I.; Bailly, C.; Mollinedo, F. DNA and non-DNA targets in the mechanism of action of the antitumor drug trabectedin. *Chem Biol* **2005,** 12, 1201-10.
22. Alvarez, C.; Alvarez, R.; Corchete, P.; Perez-Melero, C.; Pelaez, R.; Medarde, M. Exploring the effect of 2,3,4-trimethoxy-phenyl moiety as a component of indolephenstatins. *Eur J Med Chem* **2010,** 45, 588-97.
23. Jimenez, C.; Ellahioui, Y.; Alvarez, R.; Aramburu, L.; Riesco, A.; Gonzalez, M.; Vicente, A.; Dahdouh, A.; Ibn Mansour, A.; Jimenez, C.; Martin, D.; Sarmiento, R. G.; Medarde, M.; Caballero, E.; Pelaez, R. Exploring the size adaptability of the B ring binding zone of the colchicine site of tubulin with para-nitrogen substituted isocombretastatins. *Eur J Med Chem* **2015,** 100, 210-22.
24. Merry, S.; Courtney, E. R.; Fetherston, C. A.; Kaye, S. B.; Freshney, R. I. Circumvention of drug resistance in human non-small cell lung cancer in vitro by verapamil. *Br J Cancer* **1987,** 56, 401-5.
25. Rogalska, A.; Szwed, M.; Rychlik, B. The connection between the toxicity of anthracyclines and their ability to modulate the P-glycoprotein-mediated transport in A549, HepG2, and MCF-7 cells. *ScientificWorldJournal* **2014,** 2014, 819548.
26. Gaspari, R.; Prota, A. E.; Bargsten, K.; Cavalli, A.; Steinmetz, M. O. Structural Basis of *cis*- and *trans*-Combretastatin Binding to Tubulin. *Chem* **2017,** 2, 102-113.
27. Gajate, C.; Santos-Beneit, A. M.; Macho, A.; Lazaro, M.; Hernandez-De Rojas, A.; Modolell, M.; Munoz, E.; Mollinedo, F. Involvement of mitochondria and caspase-3 in ET-18-OCH(3)-induced apoptosis of human leukemic cells. *Int J Cancer* **2000,** 86, 208-18.
28. Gajate, C.; Barasoain, I.; Andreu, J. M.; Mollinedo, F. Induction of apoptosis in leukemic cells by the reversible microtubule-disrupting agent 2-methoxy-5-(2',3',4'-trimethoxyphenyl)-2,4,6-cycloheptatrien-1 -one: protection by Bcl-2 and Bcl-X(L) and cell cycle arrest. *Cancer Res* **2000,** 60, 2651-9.
29. http://www.wwpdb.org/.
30. Case, D. A.; Cheatham, T. E., 3rd; Darden, T.; Gohlke, H.; Luo, R.; Merz, K. M., Jr.; Onufriev, A.; Simmerling, C.; Wang, B.; Woods, R. J. The Amber biomolecular simulation programs. *J Comput Chem* **2005,** 26, 1668-88.
31. Alvarez, R.; Medarde, M.; Pelaez, R. New ligands of the tubulin colchicine site based on X-ray structures. *Curr Top Med Chem* **2014,** 14, 2231-52.
32. Forli, S.; Huey, R.; Pique, M. E.; Sanner, M. F.; Goodsell, D. S.; Olson, A. J. Computational protein-ligand docking and virtual drug screening with the AutoDock suite. *Nat Protoc* **2016,** 11, 905-19.
33. Morris, G. M.; Huey, R.; Lindstrom, W.; Sanner, M. F.; Belew, R. K.; Goodsell, D. S.; Olson, A. J. AutoDock4 and AutoDockTools4: Automated docking with selective receptor flexibility. *J Comput Chem* **2009,** 30, 2785-91.
34. Korb, O.; Stutzle, T.; Exner, T. E. Empirical scoring functions for advanced protein-ligand docking with PLANTS. *J Chem Inf Model* **2009,** 49, 84-96.
35. Coleman, R. G.; Carchia, M.; Sterling, T.; Irwin, J. J.; Shoichet, B. K. Ligand pose and orientational sampling in molecular docking. *PLoS One* **2013,** 8, e75992.
36. *Marvin 17.8* ChemAxon (http://www.chemaxon.com): 2017.
37. https://www.eyesopen.com/.

38. Garcia-Perez, C.; Pelaez, R.; Theron, R.; Luis Lopez-Perez, J. JADOPPT: java based AutoDock preparing and processing tool. *Bioinformatics* **2017,** 33, 583-585.